Computer Aided Geometric Design ••• (••••) •••–•••

Contents lists available at ScienceDirect

Computer Aided Geometric Design

www.elsevier.com/locate/cagd

High quality local interpolation by composite parametric surfaces

Michele Antonelli [a], Carolina Vittoria Beccari [b,*], Giulio Casciola [b]

[a] Department of Mathematics, University of Padova, Via Trieste 63, 35121 Padova, Italy
[b] Department of Mathematics, University of Bologna, Piazza di Porta San Donato 5, 40126 Bologna, Italy

ARTICLE INFO

Article history:
Received 2 December 2015
Received in revised form 17 June 2016
Accepted 18 June 2016
Available online xxxx

Keywords:
Quadrilateral mesh
Local interpolation
Non-uniform parametrization
Surface
Arbitrary topology
Curve network

ABSTRACT

In CAGD the design of a surface that interpolates an arbitrary quadrilateral mesh is definitely a challenging task. The basic requirement is to satisfy both criteria concerning the regularity of the surface and aesthetic concepts.

With regard to aesthetic quality, it is well known that interpolatory methods often produce shape artifacts when the data points are unevenly spaced. In the univariate setting, this problem can be overcome, or at least mitigated, by exploiting a proper non-uniform parametrization, that accounts for the geometry of the data. Recently the same principle has been generalized and proven to be effective in the context of bivariate interpolatory subdivision schemes.

In this paper, we propose a construction for parametric surfaces of good aesthetic quality and high smoothness interpolating quadrilateral meshes of arbitrary topology. In the classical tensor product setting the same parameter interval must be shared by an entire row or column of mesh edges. Conversely, in this paper, we assign a different parameter interval to each mesh edge. This particular structure, which we call an *augmented parametrization*, allows us to interpolate each section polyline at parameters values that prevent wiggling of the resulting curve or other interpolation artifacts and yields high quality interpolatory surfaces.

The proposed method is generalization of the local univariate spline interpolants introduced in Beccari et al. (2013a) and Antonelli et al. (2014), that have arbitrary continuity and arbitrary order of polynomial reproduction. The generated surfaces retain the same smoothness of the underlying class of univariate splines in the regular regions of the mesh (where, locally, all vertices have valence 4). Mesh regions containing vertices of valence other than 4 are covered with suitably defined surface patches joining the neighboring regular ones with G^1- or G^2-continuity.

1. Introduction

The construction of parametric curves and surfaces interpolating a given set of points is a central topic in computer-aided geometric design. In 2D, the data points are the vertices of a control polygon, whereas in 3D they are the vertices of a control polyhedron (also called a mesh). In this context, a “good” interpolant is one that faithfully mimics the shape suggested by

* Corresponding author.
E-mail addresses: antonelm@math.unipd.it (M. Antonelli), carolina.beccari2@unibo.it (C.V. Beccari), giulio.casciola@unibo.it (G. Casciola).

http://dx.doi.org/10.1016/j.cagd.2016.06.005
0167-8396/

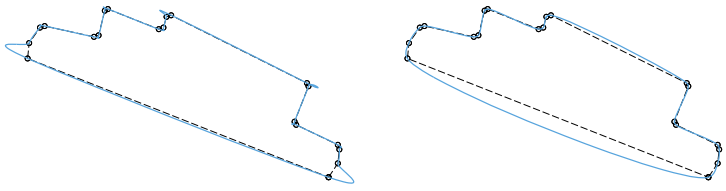

(a) Uniform parametrization (b) Centripetal parametrization

Fig. 1. Cubic (global) spline interpolation of unevenly spaced data. The uniform parametrization fails whereas a proper non-uniform parametrization yields a good interpolant.

the input data: this means, e.g., that it does not present self intersections, nor it bends to much or it is too tight in relation to the given control polygon or polyhedron.

Concerning univariate interpolation, it is well known that a proper choice of parametrization is crucial to obtain good quality curves interpolating unevenly spaced data (basic references are Farin, 2002; Farin et al., 2002). In particular, a uniform parametrization may give rise to noticeable interpolation artifacts, since it does not account for the geometry of the data. These artifacts often disappear, or are greatly mitigated, when a suitable non-uniform parametrization is used (Fig. 1 is an example).

Although there is probably no "best" parametrization, since any method can be defeated by a suitably chosen data set, some techniques produce good results in the majority of critical cases. One of the most effective (Lee, 1989; Floater, 2008; Yuksel et al., 2011), and probably the most used, is the centripetal parametrization. Alongside this, it is worth mentioning the Nielson–Foley parametrization (Foley and Nielson, 1989) and the recent method proposed in Fang and Hung (2013), which, in some cases, shows better performance than the previous ones.

Compared to global interpolation, local techniques are more prone to generating shape artifacts and, as a consequence, they suffer even more from a poor choice of parametrization. On the other hand, local methods are more efficient in that they do not involve solving systems of linear equations, which can readily be of large dimension when complex surfaces have to be generated. Moreover, editing or addition of data can be handled by updating the model only locally.

How to construct of local spline interpolants with specific properties and non-uniform parametrization has long been an open question. This could be one of the reasons why, so far, local interpolation methods have had low uptake in computer design applications. In the univariate setting, a general approach for solving the problem has been recently developed in Beccari et al. (2013a), Antonelli et al. (2014). The method allows for choosing an arbitrary support width and, correspondingly, constructing various classes of local spline interpolants that differ one from another in their degree, continuity and approximation order. In this way, one can pick the interpolating spline with properties best suited to the context of application. The popular Catmull–Rom splines (Catmull and Rom, 1974), as well as other types of previously appeared local interpolants (a non-exhaustive list includes (Chui and De Villiers, 1996; Blu et al., 2003; Becerra Sagredo, 2003; Ueno et al., 2007; Han, 2011)) are special instances of the construction.

In this paper we generalize the univariate local interpolatory splines in Beccari et al. (2013a), Antonelli et al. (2014) to the bivariate setting. Using these splines and a new parametrization technique we show how generate parametric surfaces of good aesthetic quality and high smoothness.

To achieve our goal, the main hurdle is represented by the need for defining a non-uniform parametrization that preserves the good quality of the local interpolants, when generalizing from the univariate to the bivariate setting. We shall start by considering the case of a regular mesh, where each vertex has exactly 4 incident edges. In this case, the standard approach is to construct a tensor product surface from the univariate splines that one wishes to use. Being uv the parametric domain, the tensor product requires the generation of one set of parameter values for all isoparametric curves in the u-direction; the same holds for the v-direction. For finding such a parametrization, the most reasonable way of proceeding is to create a good parametrization for each isoparametric curve using a suitable method, such as, e.g. the centripetal parametrization, and then average these parameterizations to yield one. This approach will only produce acceptable results if all the isoparametric curves essentially have the same parametrization. Conversely, when the data points significantly deviate from a regular grid, it will result in a poor choice in parameters. The isoparametric curves will unnaturally wiggle, and this defect will negatively impact the quality of the surface (see, e.g. Farin et al., 2002, §7.5.1).

The above discussion suggests that the classical idea of averaging the parametrization should be avoided. Hence we take another avenue. In particular we assign a parameter interval to each mesh edge, without requiring that the same parameter interval be shared by an entire row or column of mesh edges. We call such a parametrization an *augmented parametrization*.

A similar parametrization concept has previously been exploited in the context of subdivision schemes. It was initially proposed for Catmull–Clark surfaces (Sederberg et al., 1998; Cashman et al., 2009; Müller et al., 2006, 2010), yielding greater control over the shape of free-form objects and special features such as crease edges. In fact, the term "augmented" was firstly used in Müller et al. (2006). More recently, the augmented parametrization has also been used in the context of interpolatory subdivision schemes (Beccari et al., 2013b). The subdivision method in Beccari et al. (2013b) allows for interpolating each section polyline of the mesh at independent parameter values and generates surfaces of far superior aesthetic quality compared to their uniform or tensor-product counterparts. Unfortunately, it is subject to the typical issues of in-

Please cite this article in press as: Antonelli, M., et al. High quality local interpolation by composite parametric surfaces. Comput. Aided Geom. Des. (2016), http://dx.doi.org/10.1016/j.cagd.2016.06.005

terpolatory subdivision schemes: the resulting surfaces cannot be evaluated at arbitrary parameters and are C^1 continuous only.

The construction of the local interpolatory surfaces proposed in this paper proceeds as follows. We start by assuming that a suitable parametrization has been computed for each section polyline of the mesh. Accordingly, a different parameter interval is assigned to each mesh edge, thus yielding an augmented parametrization. Next, we choose a class of local univariate spline interpolants – based on the desired smoothness, order of polynomial reproduction and support width – and construct a composite surface that contains all the interpolatory curves of this class generated from the section polylines with the individual parameterizations. In this way, every section polyline is interpolated at the parameter values that guarantee the best quality of the resulting section curve and the generated surface turns out to be aesthetically well-behaved. We prove that, if the underlying univariate splines are C^k continuous, then the surface is globally G^k (meaning that derivatives agree after suitable reparametrization (Perters, 2002)). As a consequence, the composite surface retains the good properties of the corresponding univariate splines.

Oppositely to global interpolation techniques, the considered approach does not require to solve large systems of linear equations and allows for local editing of the generated surfaces. Moreover, unlike other local methods, it does not require to supply additional input data. Indeed, a typical drawback of local constructions, such as the popular Coons patches, is the need for prescribing cross-boundary derivatives and twist vectors, which are generally heuristically estimated. As a result only G^1 or G^2 Coons patches have been used so far, whereas the surfaces proposed in this paper can have higher continuity.

An important consequence of the locality of the proposed construction is that the method can relatively easily be extended to handle meshes with extraordinary vertices (namely vertices of valence different than 4). Applying the above interpolation scheme wherever possible (that is away from the extraordinary vertices) will generate a surface with "holes" around the extraordinary vertices. Across the boundary of such holes, the tangent field (and higher order derivative fields) are determined by the surrounding regular patches and, as a consequence of the augmented parametrization, they change at every boundary point in a peculiar way. The missing part of the surface shall be defined in such a way to interpolate the existing derivative fields up to reasonable order of continuity.

The general problem of how to fill the hole around an extraordinary vertex is an active research topic even in the case of uniform parametrization. Recent developments include Várady et al. (2011), Salvi et al. (2014), Salvi and Várady (2014), where transfinite multi-sided patches are generated by interpolating derivative ribbons. Moreover, a whole branch of research is devoted to the problem of filling an n-sided hole in a tensor product bi-cubic spline surface. Early constructions, such as Prautzsch (1997), produce a G^2 covering of the hole by bi-sextic surface patches, but are not focused on shape quality. To generate aesthetically well-behaved G^2 splines, a bi-septic construction based on minimizing a suitable energy functional is presented in Loop and Schaefer (2008). In Karčiauskas and Peters (2015) a G^1 piecewise bi-quintic surface patch is developed to fill the n-sided hole in a piecewise bi-cubic tensor-product spline surface with optimized curvature distribution.

Our main point here is not to provide a one-stop solution, but to demonstrate how to obtain good quality local interpolating surfaces by exploiting, in synergy, the augmented parametrization, the regular patches described above and a local patching scheme for extraordinary vertices. We will address this issue by mans of either G^1 Coons–Gregory patches (Gregory, 1974; Hoschek and Lasser, 1993; Farin, 2002) and their G^2 version (Miura and Wang, 1991; Hermann, 1996). In both cases, we will see how to suitably tweak the definition of the patches, in order to interpolate the desired boundary information. This will allow us to generate augmented surfaces that interpolate a mesh containing extraordinary vertices, have arbitrary smoothness in the regular regions, and are G^1 or G^2 continuous in the extraordinary regions.

We would like to remark that the research reported in this paper was supported by the European Eurostars project NIIT4CAD, aimed at the development of new technologies for modeling arbitrary topology surfaces within CAD systems. One of the advanced objectives of the project was to construct local interpolatory surfaces suitable for integration in a CAD system and this paper is a part of such a study.

The remainder of the paper is organized as follows. In Section 2 we recall the univariate local spline interpolants presented in Beccari et al. (2013a), Antonelli et al. (2014). For regular input meshes, in Section 3 we introduce the augmented parametrization and the construction of local interpolatory surfaces, also discussing their relevant properties. Section 3.1 presents some application examples to demonstrate the effectiveness of the method and its better performance compared to the classical tensor product approach. In Section 4 we address the problem of patching the extraordinary regions of the mesh by G^1 and G^2 augmented Coons–Gregory patches. Section 4.3 illustrates a possible approach to generate the boundary curves and cross-boundary derivative fields needed for the definition of these patches, when this information is not available. Section 4.4 presents examples of augmented surfaces containing extraordinary vertices and finally Section 5 summarizes the results achieved and suggests some topics for future research.

2. Local, non-uniform, univariate spline interpolation

Given a sequence of points $\boldsymbol{p}_0, \boldsymbol{p}_1, \ldots, \boldsymbol{p}_N$ in $\mathbb{R}^n$, $n \geq 2$, where $\boldsymbol{p}_j$ and $\boldsymbol{p}_{j+1}$ are distinct and $\boldsymbol{p}_N = \boldsymbol{p}_0$, and an associated sequence of parameter values $x_0 < x_1 < \cdots < x_N$, we consider the periodic spline curve $\boldsymbol{F} : [x_0, x_N] \to \mathbb{R}^n$ defined as

$$\boldsymbol{F}(x) = \sum_i \boldsymbol{p}_i \, \psi_i(x). \tag{1}$$

Please cite this article in press as: Antonelli, M., et al. High quality local interpolation by composite parametric surfaces. Comput. Aided Geom. Des. (2016), http://dx.doi.org/10.1016/j.cagd.2016.06.005

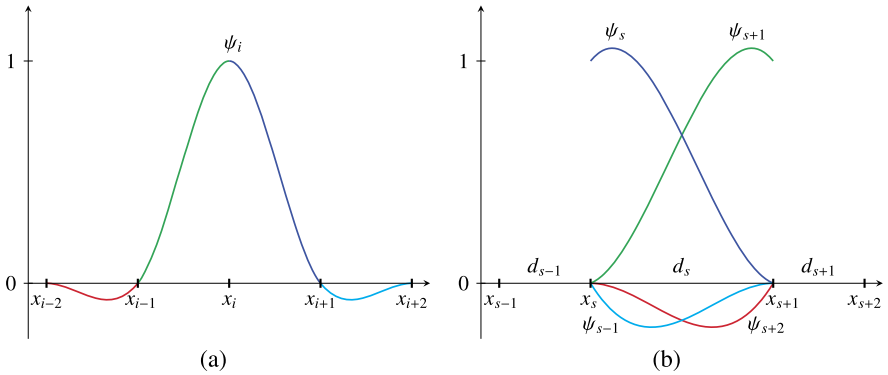

Fig. 2. (a) Fundamental function ψ_i of the class $D^3C^1P^2S^4$, with the different pieces represented in different colors. (b) The fundamental functions of the class $D^3C^1P^2S^4$ that are nonzero in the interval $[x_s, x_{s+1}]$. (For interpretation of the references to color in this figure, the reader is referred to the web version of this article.)

In the above formula, $\psi_i : [x_0, x_N] \to \mathbb{R}$ are *fundamental spline functions*, namely they are piecewise functions on the partition $\{x_j\}$ such that $\psi_i(x_j) = \delta_{i,j}$. Since we are interested in local interpolation, we require that every ψ_i has compact support, namely that it is nonzero in a finite number of parametric intervals. In this way, when the data points are in $\mathbb{R}^n$, $n = 2, 3$, formula (1) represents a parametric curve that locally interpolates the given data.

In the remainder of the paper, we suppose that the fundamental functions ψ_i have even support width w, namely

$$\psi_i(x) = 0, \qquad x \notin [x_{i-\frac{w}{2}}, x_{i+\frac{w}{2}}].$$

This assumption guarantees that the interpolating splines in (1) preserve possible symmetries in the data and allows us to consistently simplify the notation that will be introduced later on.

Confining ourselves to polynomial splines, the characterizing properties of the fundamental functions are degree, continuity, maximum degree of polynomials that can be reproduced (this is equal to the approximation order minus one) and support width. Obviously, these properties of are inherited by the parametric interpolant $\boldsymbol{F}$.

A general method for constructing local interpolatory splines with specific properties and non-uniform parametrization has recently been developed in the Beccari et al. (2013a), Antonelli et al. (2014). In that framework, we can choose an arbitrary support width and, correspondingly, construct various classes of spline interpolants of the form (1) that differ one from another in their degree, continuity and approximation order. Special instances of such splines are Catmull–Rom splines (Catmull and Rom, 1974), as well as other types of local interpolants including those in Chui and De Villiers (1996), Blu et al. (2003), Becerra Sagredo (2003), Ueno et al. (2007), Han (2011). Adopting the notation in Beccari et al. (2013a), Antonelli et al. (2014), we indicate a class of splines having Degree g, Continuity order k, Polynomial reproduction degree m and Support width w by the shorthand notation $D^gC^kP^mS^w$. Tables 1, 2, and 3 in Beccari et al. (2013a) and Table 2 in Antonelli et al. (2014) summarize the different classes that we can construct for the most usual choices of support width, namely 4, 6 and 8. Some examples with $w = 4$ include the families $D^3C^0P^3S^4$, $D^3C^1P^2S^4$, $D^4C^2P^1S^4$, $D^5C^2P^2S^4$ from Beccari et al. (2013a) and $D^2C^1P^2S^4$ or $D^3C^2P^2S^4$ from Antonelli et al. (2014). Even more families of splines can be found widening the support width to 6 or 8.

We now introduce a convenient notation, emphasizing the local dependence on data and parameters, which will be useful in generalizing the above framework to the bivariate case. To this aim, we shall observe that in each parametric interval there are exactly w nonzero fundamental functions, each of which depends on a sequence of $w - 1$ *parameter intervals* of the form

$$d_i = x_{i+1} - x_i. \tag{2}$$

As a consequence, the vector

$$\boldsymbol{d} = \left(d_{s-\frac{w}{2}+1}, \ldots, d_s, \ldots, d_{s+\frac{w}{2}-1}\right), \tag{3}$$

contains all the information necessary to evaluate $\boldsymbol{F}$ in $[x_s, x_{s+1}]$. We call such a vector the *local parameter vector* relative to $[x_s, x_{s+1}]$ (or, equivalently, relative to $\overline{\boldsymbol{p}_s\boldsymbol{p}_{s+1}}$). Mapping the interval $[x_s, x_{s+1}]$ to $[0, d_s]$, the segment of $\boldsymbol{F}$ bounded by $\boldsymbol{p}_s$ and $\boldsymbol{p}_{s+1}$ can now be written as

$$\boldsymbol{F}(x)\big|_{[0,d_s]} = \sum_{i=s-\frac{w}{2}+1}^{s+\frac{w}{2}} \boldsymbol{p}_i\, \psi_i(x, \boldsymbol{d}), \tag{4}$$

where $\psi_i(x, \boldsymbol{d})$ is the restriction of $\psi_i(x)$ to $[x_s, x_{s+1}]$ expressed in terms of the sequence of parameter intervals (3).

Please cite this article in press as: Antonelli, M., et al. High quality local interpolation by composite parametric surfaces. Comput. Aided Geom. Des. (2016), http://dx.doi.org/10.1016/j.cagd.2016.06.005

As an example of our setting and notation, we provide in Appendix A the expressions for the well-known Catmull–Rom splines (Catmull and Rom, 1974), corresponding to the class $D^3C^1P^2S^4$ in Beccari et al. (2013a), also represented in Fig. 2. To facilitate the reader in reproducing the examples proposed in the following sections, we also list in appendix the fundamental functions $D^5C^2P^2S^4$. The latter are an interesting application of the approach in Beccari et al. (2013a), since they have high continuity, in spite of a very limited support. Moreover, given our focus on interpolating 3-dimensional data, it may also be useful to consider splines with continuity C^3, or higher, and some graphical examples will be presented in the forthcoming sections. As it can reasonably be expected, in this case the explicit expression of the fundamental functions is more complicated. Nevertheless, the evaluation of a spline interpolant can still be performed in a computationally efficient way as discussed in Beccari et al. (2013a), Antonelli et al. (2014).

As recalled in the previous section, the choice of the parameter sequence $\{x_j\}$ has a large influence on the shape of an interpolating spline curve and various and effective methods to automatically compute the values $\{x_j\}$ exist, such as Ahlberg et al. (1967), Lee (1989), Foley and Nielson (1989), Fang and Hung (2013). Since the focus of this paper is not on comparing different parametrization techniques, we will make use of the centripetal parametrization, which is acknowledged to produce good results for the majority of critical data sets. According to the centripetal parametrization, fixed x_0, the subsequent x_j, $j = 1, \ldots, N$ are computed through

$$x_{i+1} = x_i + \left\| \boldsymbol{p}_{i+1} - \boldsymbol{p}_i \right\|_2^{\alpha}, \tag{5}$$

with $\alpha = \frac{1}{2}$ and $\|\cdot\|_2$ denoting the Euclidean norm. It is therefore clear that the parameter values depend on the geometry of the interpolation points. From (5), the chordal and uniform parameterizations can also be obtained by setting respectively $\alpha = 1$ and $\alpha = 0$ (Farin, 2002; Farin et al., 2002).

In the following section we generalize the considered interpolants to the bivariate setting. Before proceeding, we need to remark that our assumption to work with periodic data has the sole purpose of simplifying the presentation. Open curves can similarly be defined, provided that "special" fundamental functions are used in order to evaluate (1) in the boundary intervals (Antonelli et al., 2014). These fundamental functions can be determined so as to interpolate the derivatives of $\boldsymbol{F}$ up to suitable order at x_0 and x_N. The surface construction developed in the following section can be adapted to handle open data sets along the same lines of the univariate case.

3. Local interpolation of regular meshes by high quality surfaces with arbitrary continuity

In this section we develop a local method to generate interpolatory surfaces of good quality and high order of continuity from regular input meshes. In the present context, a surface of "good quality" is one that faithfully resembles the shape suggested by the input data and does not present undesired interpolation artifacts. The approach is based on the previously recalled univariate spline interpolants and on a proper technique of parametrization. As will be proved in the following, the resulting surfaces are G^k-continuous when constructed upon a class of fundamental functions of type $D^gC^kP^gS^w$.

A regular mesh is one where every vertex belongs to four edges (and faces) and can thus be seen as a rectangular grid of 3D points, whose edges are associated with two independent domain directions. We say that two edges are *opposite* when they have no vertex in common and they belong to the same face, whereas we say that two edges are *adjacent* when they have one vertex in common and do not belong to the same face. We call an *edge ribbon* any ordered sequence of pairwise opposite edges and a *section polyline* a polyline formed by a sequence of pairwise adjacent edges. Moreover, we call a *section curve* any curve interpolating the vertices of a section polyline. For simplicity, the discussion will be limited to meshes without boundary and therefore we can assume that all section polylines and curves are closed.

In the Introduction, we have drawn the reader's attention the well-known fact that a tensor-product surface may easily yield poor-quality interpolants. This is because all isocurves of such a surface must have the same parametrization. As recalled, the latter requirement may result in an unnatural wiggling of the section curves that is very likely to happen when the data points are unevenly spaced and is even more evident when local interpolation methods are used.

In contrast to the tensor product technique, we wish to construct a surface where the vertices of each section polyline are interpolated at the parameter values that allow for the best quality of the resulting section curve.

To this aim, for every section polyline, we derive a non-uniform parameter sequence by exploiting an appropriate data-dependent technique of parametrization. Then we assign to the section polyline edges the resulting parameter intervals. For instance, labeled by $\boldsymbol{p}_{i,j}$ the mesh points, the centripetal parametrization applied to every section polyline will produce the edge parameter intervals

$$d_{i,j} := \left\| \boldsymbol{p}_{i+1,j} - \boldsymbol{p}_{i,j} \right\|_2^{\alpha} \qquad \text{and} \qquad e_{i,j} := \left\| \boldsymbol{p}_{i,j+1} - \boldsymbol{p}_{i,j} \right\|_2^{\alpha}, \qquad \alpha = \frac{1}{2}. \tag{6}$$

This can easily be seen comparing the above expressions and formulae (2)–(5).

We call the resulting configuration of parameters an *augmented parametrization*. The augmented parametrization is featured by the fact that the parameter intervals allocated to the edges of one mesh face will not form, in general, a rectangle. Conversely, in a tensor product surface, the parameter intervals must be equal for all edges belonging in the same edge ribbon, or, equivalently, the intervals allocated to the edges of every mesh face must form a rectangle.

We now aim to construct a composite surface, which we call an *augmented surface*, where every section curve is a local, univariate, spline of class $D^gC^kP^mS^w$ and has an independent parametrization determined by the edge parameter intervals

Please cite this article in press as: Antonelli, M., et al. High quality local interpolation by composite parametric surfaces. Comput. Aided Geom. Des. (2016), http://dx.doi.org/10.1016/j.cagd.2016.06.005

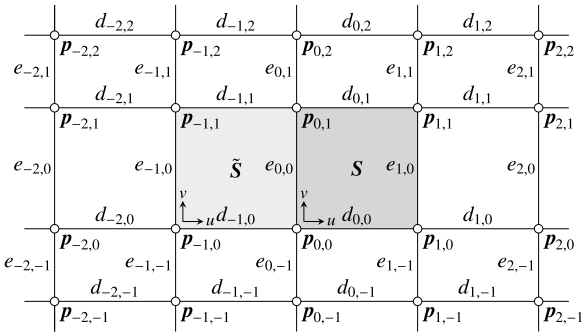

Fig. 3. Labeling of vertices and parameter intervals for the construction of the augmented surface patch $\boldsymbol{S}$ having the expression (10).

of the corresponding section polyline. This means that the section curve piece bounded by $\boldsymbol{p}_{i,j}$ and $\boldsymbol{p}_{i+1,j}$ should have an associated parametric interval of length equal to $d_{i,j}$. Analogously, the parametric interval between any two vertices, $\boldsymbol{p}_{i,j}$ and $\boldsymbol{p}_{i,j+1}$ of the corresponding section curve should have length $e_{i,j}$. In this way, each section polyline of the mesh can be interpolated at the parameter values that allow the best quality of the resulting section curve. As a consequence, the surface passing through these curves will most likely be aesthetically well-behaved.

It is sufficient to illustrate the construction for a generic surface patch interpolating the points $\boldsymbol{p}_{s,t}$, $\boldsymbol{p}_{s+1,t}$, $\boldsymbol{p}_{s,t+1}$, $\boldsymbol{p}_{s+1,t+1}$ and in particular, without loss of generality, we can consider the one which interpolates $\boldsymbol{p}_{0,0}$, $\boldsymbol{p}_{1,0}$, $\boldsymbol{p}_{0,1}$, $\boldsymbol{p}_{1,1}$, depicted in Fig. 3. (As of now, the neighboring patch $\tilde{\boldsymbol{S}}$ in Fig. 3 shall be overlooked. It will be used later in the proof of Proposition 2.) Any other patch can be analogously derived by proper index shift.

Let $[0,1]^2$ be the parametric domain associated with the considered patch. The first stage of the construction is to choose a class of local, univariate, spline interpolants $D^g C^k P^m S^w$, based on the properties that we seek in the final surface. Hence, in view of the C^k continuity of the fundamental functions, we consider the polynomials $\delta_{i,j}(v)$ $i=-\frac{w}{2}+1,\dots,\frac{w}{2}-1$, $j=0$ and $\epsilon_{i,j}(u)$ $i=0$, $j=-\frac{w}{2}+1,\dots,\frac{w}{2}-1$, of degree $2k+1$, uniquely determined by the following conditions:

$$\begin{aligned}
&\delta_{i,j}:[0,1]\to[d_{i,j},d_{i,j+1}],\\
&\delta_{i,j}(0)=d_{i,j}, \qquad \text{and} \qquad \delta_{i,j}(1)=d_{i,j+1},\\
&\delta_{i,j}^{(r)}(0)=\delta_{i,j}^{(r)}(1)=0, \qquad r=1,\dots,k,
\end{aligned} \tag{7a}$$

and

$$\begin{aligned}
&\epsilon_{i,j}:[0,1]\to[e_{i,j},e_{i+1,j}],\\
&\epsilon_{i,j}(0)=e_{i,j}, \qquad \text{and} \qquad \epsilon_{i,j}(1)=e_{i+1,j},\\
&\epsilon_{i,j}^{(r)}(0)=\epsilon_{i,j}^{(r)}(1)=0, \quad r=1,\dots,k.
\end{aligned} \tag{7b}$$

We call the above polynomials $\delta_{i,j}$ and $\epsilon_{i,j}$ the *local parametrization functions*. Since $\delta_{i,j}(v)$ and $\epsilon_{i,j}(u)$ have vanishing derivatives up to order k at 0 and 1, they are monotonic functions with positive first derivative. Moreover they interpolate the two parameter intervals corresponding to opposite edges of a mesh face and therefore have the effect of "blending" the parametrizations. As it will become clear later on, this property is fundamental in guaranteeing that the section polylines of the surface be interpolated at the initially assigned parameter intervals.

We use the local parametrization functions to associate two local parameter vectors $\boldsymbol{d}$ and $\boldsymbol{e}$ with any $(u,v)\in[0,1]^2$. In particular, let us set:

$$\boldsymbol{d}=\boldsymbol{d}(v)=\left(\delta_{-\frac{w}{2}+1,0}(v),\dots,\delta_{0,0}(v),\dots\delta_{\frac{w}{2}-1,0}(v)\right), \tag{8a}$$

and

$$\boldsymbol{e}=\boldsymbol{e}(u)=\left(\epsilon_{0,-\frac{w}{2}+1}(u),\dots,\epsilon_{0,0}(u),\dots,\epsilon_{0,\frac{w}{2}-1}(u)\right). \tag{8b}$$

In this way, at the patch boundary described by $(u,0)$, $u\in[0,1]$, $\boldsymbol{d}=\left(d_{-w/2+1,0},\dots,d_{0,0},\dots,d_{w/2-1,0}\right)$ is the local parameter vector relative to $\overline{\boldsymbol{p}_{0,0}\boldsymbol{p}_{1,0}}$ (see its definition in (3)). In addition, at the opposite boundary $(u,1)$, $\boldsymbol{d}$ is the local parameter vector relative to $\overline{\boldsymbol{p}_{0,1}\boldsymbol{p}_{1,1}}$. Analogously, for any point $(0,v)$ or $(1,v)$, $v\in[0,1]$, $\boldsymbol{e}$ is the local parameter vector associated respectively with $\overline{\boldsymbol{p}_{0,0}\boldsymbol{p}_{0,1}}$ or $\overline{\boldsymbol{p}_{1,0}\boldsymbol{p}_{1,1}}$.

We also consider the two *local variables*

$$x=u\,\delta_{0,0}(v), \qquad \text{and} \qquad y=v\,\epsilon_{0,0}(u), \tag{9}$$

such that x and y span the intervals $[0,\delta_{0,0}(v)]$ and $[0,\epsilon_{0,0}(u)]$ while respectively u and v vary in $[0,1]$.

Please cite this article in press as: Antonelli, M., et al. High quality local interpolation by composite parametric surfaces. Comput. Aided Geom. Des. (2016), http://dx.doi.org/10.1016/j.cagd.2016.06.005

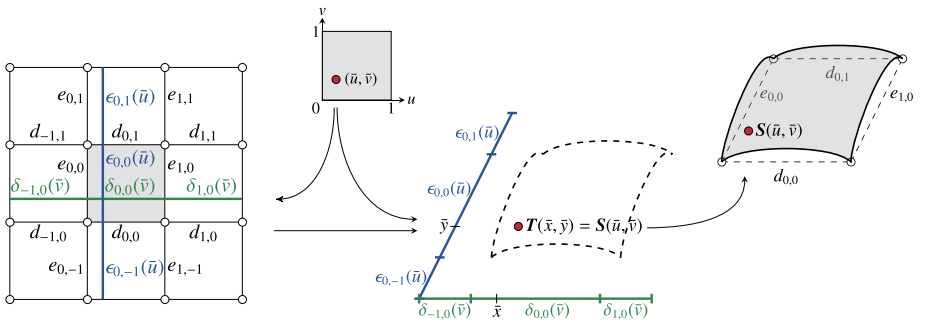

Fig. 4. Construction of an augmented patch in the case of support width $w = 4$.

Finally, for any $(u, v) \in [0, 1]^2$, we define the augmented surface patch $\boldsymbol{S}$ by

$$\boldsymbol{S}(u, v) = \sum_{i=-\frac{w}{2}+1}^{\frac{w}{2}} \sum_{j=-\frac{w}{2}+1}^{\frac{w}{2}} \boldsymbol{p}_{i,j} \Psi_{i,j}\Big(x, y, \boldsymbol{d}, \boldsymbol{e}\Big), \tag{10}$$

where

$$\Psi_{i,j}\Big(x, y, \boldsymbol{d}, \boldsymbol{e}\Big) = \psi_i\Big(x, \boldsymbol{d}\Big)\, \psi_j\Big(y, \boldsymbol{e}\Big), \tag{11}$$

with local parameter vectors $\boldsymbol{d}, \boldsymbol{e}$ given by (8a)–(8b) and x, y computed through (9).

Note that $\boldsymbol{S}$ depends on a grid of mesh vertices of size equal to $w \times w$, where w is the support width of the underlying functions ψ_i and ψ_j. For brevity, we will sometimes say that the patch has support w.

Remark 1. For simplicity of presentation we have assumed that the functions $\psi_i(x, \boldsymbol{d})$ and $\psi_j(y, \boldsymbol{e})$ in (11) belong to the same family $D^g C^k P^m S^w$. However, the construction can easily be adapted to allow fundamental functions of two different classes $D^g C^k P^m S^w$.

We remark that the augmented patch $\boldsymbol{S}$ is not a tensor product surface. More precisely, we can interpret the above construction as follows. For a given $(\bar{u}, \bar{v}) \in [0, 1]^2$, let $\bar{\boldsymbol{d}}$ and $\bar{\boldsymbol{e}}$ be the vectors

$$\bar{\boldsymbol{d}} = \boldsymbol{d}(\bar{v}), \quad \bar{\boldsymbol{e}} = \boldsymbol{e}(\bar{u}),$$

computed through (8a)–(8b), and let $\bar{d} = \delta_{0,0}(\bar{v})$ and $\bar{e} = \epsilon_{0,0}(\bar{u})$. Then the value of $\boldsymbol{S}$ at $(\bar{u}, \bar{v})$ is obtained by evaluating the tensor product patch

$$\boldsymbol{T}_{(\bar{u},\bar{v})}(x, y) = \sum_{i=-\frac{w}{2}+1}^{\frac{w}{2}} \sum_{j=-\frac{w}{2}+1}^{\frac{w}{2}} \boldsymbol{p}_{i,j} \psi_i\Big(x, \bar{\boldsymbol{d}}\Big)\, \psi_j\Big(y, \bar{\boldsymbol{e}}\Big), \qquad (x, y) \in [0, \bar{d}] \times [0, \bar{e}],$$

at the point $(\bar{x}, \bar{y})$, namely by setting $\boldsymbol{S}(\bar{u}, \bar{v}) = \boldsymbol{T}_{(\bar{u},\bar{v})}(\bar{x}, \bar{y})$. In this view, a different tensor-product patch $\boldsymbol{T}_{(\bar{u},\bar{v})}$ determines the value of $\boldsymbol{S}$ at each domain point $(\bar{u}, \bar{v}) \in [0, 1]^2$.

The construction of the augmented surface patch $\boldsymbol{S}$ is schematized in Fig. 4 for a class of fundamental functions having support width $w = 4$ and, more generally, can be summarized as follows. Each mesh face gives rise to a surface patch, parameterized over the domain $[0, 1]^2$. For a given $(\bar{u}, \bar{v}) \in [0, 1]^2$ we locally interpolate the parameter intervals, separately in the u and v direction, in order to generate two local parameter vectors $\bar{\boldsymbol{d}} = \boldsymbol{d}(\bar{v})$ and $\bar{\boldsymbol{e}} = \boldsymbol{e}(\bar{u})$. We also map $(\bar{u}, \bar{v})$ into a couple of values $(\bar{x}, \bar{y})$. This mapping is such that, at the boundaries $(u, 0)$ and $(u, 1)$, $u \in [0, 1]$, x spans respectively the entire intervals $[0, d_{0,0}]$ and $[0, d_{0,1}]$. Analogously, at the boundaries $(0, v)$ and $(1, v)$, $v \in [0, 1]$, y spans respectively the intervals $[0, e_{0,0}]$ and $[0, e_{1,0}]$. These are precisely the parameter intervals allocated to the edges of the given mesh face. Finally, we consider the surface $\boldsymbol{T}_{(\bar{u},\bar{v})}(x, y)$ defined as tensor product of the local univariate fundamental functions of class $D^g C^k P^m S^w$ on $\bar{\boldsymbol{d}}$ and $\bar{\boldsymbol{e}}$ and we set $\boldsymbol{S}(\bar{u}, \bar{v}) = \boldsymbol{T}_{(\bar{u},\bar{v})}(\bar{x}, \bar{y})$.

The remainder of this section is devoted to showing that the resulting composite surface has all the sought properties. We start by proving that the surface section curves form a network of univariate spline interpolants of class $D^g C^k P^m S^w$, where each curve has an independent non-uniform parametrization determined by the edge parameter intervals of the corresponding section polyline. In other words, if a network of section curves of class $D^g C^k P^m S^w$ was independently determined before constructing the surface, then the surface would precisely be a transfinite interpolant of these curves.

Proposition 1. *The section curves of an augmented surface based on a class of fundamental functions $D^g C^k P^m S^w$ are local univariate splines in the same class.*

Please cite this article in press as: Antonelli, M., et al. High quality local interpolation by composite parametric surfaces. Comput. Aided Geom. Des. (2016), http://dx.doi.org/10.1016/j.cagd.2016.06.005

Proof. It suffices to show that the section curve segment bounded by $\boldsymbol{p}_{0,1}$ and $\boldsymbol{p}_{1,1}$ (see Fig. 3) belongs to the unique local, non-uniform spline curve $\boldsymbol{F}$ of class $D^gC^kP^mS^w$ interpolating the section polyline with vertices $\ldots, \boldsymbol{p}_{-1,1}, \boldsymbol{p}_{0,1}, \boldsymbol{p}_{1,1}, \boldsymbol{p}_{2,1}\cdots$ and parameter intervals $\ldots, d_{-1,1}, d_{0,1}, d_{1,1}, d_{2,1}\ldots$. Hence the statement can immediately be extended to the entire network of section curves.

According to the local representation (4), we have

$$\boldsymbol{F}(x) = \sum_{i=-\frac{w}{2}+1}^{\frac{w}{2}} \boldsymbol{p}_{i,1}\,\psi_i(x, \bar{\boldsymbol{d}}), \quad x \in [0, d_{0,1}], \tag{12}$$

with local parameter vector

$$\bar{\boldsymbol{d}} = \left(d_{-\frac{w}{2}+1,1}, \ldots, d_{0,1}, \ldots, d_{\frac{w}{2}-1,1}\right).$$

The patch boundary with endpoints $\boldsymbol{p}_{0,1}$ and $\boldsymbol{p}_{1,1}$ is described by (10) for $u \in [0,1]$, $v = 1$. At any such point (u, v), the fundamental functions ψ_j of the class $D^gC^kP^mS^w$, $j = -w/2+1, \ldots, w/2-1$, have the values $\psi_1(y, \boldsymbol{e}) = 1$ and $\psi_j(y, \boldsymbol{e}) = 0$, for any $j \neq 1$, and, by (9), $x = ud_{0,1}$. Substituting in (10) we get

$$\boldsymbol{S}(u, 1) = \sum_{i=-\frac{w}{2}+1}^{\frac{w}{2}} \boldsymbol{p}_{i,1}\psi_i(x, \boldsymbol{d}).$$

Hence, the statement follows by observing that the local parameter vectors $\boldsymbol{d}$ and $\bar{\boldsymbol{d}}$ are equal and thus the curve segments determined by the above formula and by (12) are identical. □

We shall now study the continuity of an augmented composite surface. Preliminarily, we observe that each surface patch is defined as a composition of infinitely differentiable functions (note that the edge parameter intervals are assumed to be nonzero). Moreover, Proposition 1 guarantees the continuity of the constructed surface and entails that two neighboring augmented patches have C^k continuous derivatives in the direction of their common boundary. The following proposition shows that the same smoothness holds in the cross-boundary direction and in particular allows us to conclude that the constructed surface is globally G^k continuous.[1] For ease of notation, we formulate the statement for the two patches $\boldsymbol{S}$ and $\tilde{\boldsymbol{S}}$ represented in Fig. 3. It is immediate to see that the result holds when considering any two neighboring patches and their common boundary, provided appropriate adjustment of indices.

Proposition 2. *Let $\boldsymbol{S}$ and $\tilde{\boldsymbol{S}}$ be the two adjacent augmented surface patches depicted in Fig. 3, based on fundamental functions of class $D^gC^kP^mS^w$. Then the derivatives across their common boundary satisfy the relation*

$$\frac{\partial^r}{\partial u^r}\boldsymbol{S}(u, v)|_{(0,v)} = \Delta^r(v)\frac{\partial^r}{\partial u^r}\tilde{\boldsymbol{S}}(u, v)|_{(1,v)}, \qquad r = 0, \ldots, k, \tag{13}$$

where

$$\Delta(v) = \frac{\delta_{0,0}(v)}{\delta_{-1,0}(v)}, \tag{14}$$

and $\delta_{0,0}$ and $\delta_{-1,0}$ are the local parametrization functions defined in (7a).

The above result can be shown by direct verification, and we postpone the proof to the end of this section. For the moment, it is important to observe that relation (14) provides the scaling $\Delta(v)$ relating the cross-boundary derivatives of $\boldsymbol{S}$ and $\tilde{\boldsymbol{S}}$. In general, $\Delta(v)$ is different at each boundary point, but varies smoothly along the boundary, being defined as the ratio of two positive polynomials. As a consequence of Proposition 2 we obtain the following result.

Proposition 3. *Two augmented surface patches built upon a class of fundamental functions $D^gC^kP^mS^w$ join along their common boundary with G^k-continuity.*

Proof. Without loss of generality, we can take the two patches $\boldsymbol{S}$ and $\tilde{\boldsymbol{S}}$ in Proposition 2 and consider the map

$$\boldsymbol{\rho}(u, v) = \begin{pmatrix} \Delta(v)u + 1 \\ v \end{pmatrix},$$

[1] G^k continuity refers to agreement of derivatives after suitable reparametrization (Perters, 2002).

Please cite this article in press as: Antonelli, M., et al. High quality local interpolation by composite parametric surfaces. Comput. Aided Geom. Des. (2016), http://dx.doi.org/10.1016/j.cagd.2016.06.005

where $\Delta(v)$ is given by (14). The function $\boldsymbol{\rho}$ is a C^k reparametrization between the two domains of $\boldsymbol{S}$ and $\tilde{\boldsymbol{S}}$. Moreover, exploiting relation (13), it is immediate to verify that

$$\frac{\partial^r}{\partial u^r}\boldsymbol{S}(u,v)|_{(0,v)} = \frac{\partial^r}{\partial u^r}\left(\tilde{\boldsymbol{S}}\circ\boldsymbol{\rho}\right)(u,v)|_{(0,v)}, \qquad r=0,\dots,k.$$

The above observations entail that the two considered patches join along their common boundary with G^k-continuity. □

The remainder of this section is devoted to proving Proposition 2. As a premise, the following Lemma is stated as an independent result, since it will be later recalled in Section 4.

Lemma 1. *Let $\boldsymbol{S}$ be an augmented surface patch of the form (10). Then its cross-boundary derivatives satisfy the following relations*

$$\begin{aligned}\frac{\partial^r}{\partial u^r}\boldsymbol{S}(u,v)|_{(\bar{u},v)} &= \frac{\partial^r}{\partial x^r}\boldsymbol{S}\Big(x,y,\boldsymbol{d},\boldsymbol{e}\Big)|_{(\bar{u},v)}\delta^r_{0,0}(v), \quad \bar{u}=0,1,\\ \frac{\partial^r}{\partial v^r}\boldsymbol{S}(u,v)|_{(u,\bar{v})} &= \frac{\partial^r}{\partial y^r}\boldsymbol{S}\Big(x,y,\boldsymbol{d},\boldsymbol{e}\Big)|_{(u,\bar{v})}\epsilon^r_{0,0}(u), \quad \bar{v}=0,1,\end{aligned} \tag{15}$$

where $\delta_{0,0}$ and $\epsilon_{0,0}$ are the local parametrization functions defined in (7a)–(7b).

Proof. The result immediately follows by using the chain rule, relation (9) and the fact that $\delta^{(r)}_{i,0}(v) = \epsilon^{(r)}_{0,j}(u) = 0$, $r = 1,\dots,k$, $u,v=0,1$ and $i,j=-\frac{w}{2}+1,\dots,\frac{w}{2}-1$. □

The above result relies on the fact that the local parametrization functions (7a)–(7b) have vanishing derivatives at the endpoints of their interval of definition. As we will see shortly, this property also plays a prominent role in proving Proposition 2. An interesting consequence is that, in order to prescribe a correct set of local parametrization functions, it is not sufficient to require that these functions interpolate the edge parameter intervals values. Indeed, the aforementioned condition on the derivatives is essential to guarantee that the composite surface be G^k continuous.

Proof of Proposition 2. Without loss of generality, we can assume that the local reference system uv of the two patches is oriented as illustrated in Fig. 3. Therefore, the common boundary of $\boldsymbol{S}$ and $\tilde{\boldsymbol{S}}$ corresponds to $(0,v)$ for $\boldsymbol{S}$ and $(1,v)$ for $\tilde{\boldsymbol{S}}$. We refer to the same figure for the labeling of all the relevant quantities involved. To prove the statement, we shall verify that (13)–(14) hold for any arbitrary $v\in[0,1]$.

By differentiating formulae (10)–(11) in the cross-boundary direction u, we obtain

$$\frac{\partial^r}{\partial u^r}\boldsymbol{S}(u,v) = \sum_{i=-\frac{w}{2}+1}^{\frac{w}{2}}\sum_{j=-\frac{w}{2}+1}^{\frac{w}{2}}\boldsymbol{p}_{i,j}\sum_{q=0}^{r}\binom{r}{q}\frac{\partial^q}{\partial u^q}\psi_i\Big(u\delta_{0,0}(v),\boldsymbol{d}(v)\Big)\frac{\partial^{r-q}}{\partial u^{r-q}}\psi_j\Big(v\epsilon_{0,0}(u),\boldsymbol{e}(u)\Big), \tag{16}$$

where

$$\boldsymbol{d}(v) = \Big(\delta_{-\frac{w}{2}+1,0}(v),\dots,\delta_{0,0}(u),\dots,\delta_{\frac{w}{2}-1,0}(v)\Big) \qquad \text{and} \qquad \boldsymbol{e}(u) = \Big(\epsilon_{0,-\frac{w}{2}+1}(u),\dots,\epsilon_{0,0}(u),\dots,\epsilon_{0,\frac{w}{2}-1}(u)\Big). \tag{17}$$

From the definition of the local parametrization functions in (7a)–(7b), we have $\epsilon'_{h,0}(0)=0$, $h=-\frac{w}{2}+1,\dots,\frac{w}{2}-1$ and therefore

$$\frac{\partial}{\partial u}\psi_j\Big(v\epsilon_{0,0}(u),\boldsymbol{e}(u)\Big)\Big|_{(0,v)} = \sum_{h=-\frac{w}{2}+1}^{\frac{w}{2}-1}\frac{\partial\psi_j}{\partial\epsilon_{h,0}}\frac{\partial\epsilon_{h,0}}{\partial u}\Big|_{(0,v)} = 0.$$

Moreover, since $\epsilon^{(r)}_{h,0}(u)$ vanishes at $u=0$, for all $r=1,\dots,k$, by iterating the differentiation process (cf. Faà di Bruno's law) it can be easily verified that

$$\frac{\partial^{r-q}}{\partial u^{r-q}}\psi_j\Big(v\epsilon_{0,0}(u),\boldsymbol{e}(u)\Big)\Big|_{(0,v)} = 0, \qquad q=0,\dots,r-1, \qquad r=1,\dots,k.$$

In addition, recalling that the fundamental functions $D^gC^kP^mS^w$ have continuity C^k and support width w, there holds

$$\frac{\partial^r}{\partial u^r}\psi_{\frac{w}{2}}\Big(u\delta_{0,0}(v),\boldsymbol{d}(v)\Big)\Big|_{(0,v)} = 0, \qquad r=1,\dots,k.$$

Please cite this article in press as: Antonelli, M., et al. High quality local interpolation by composite parametric surfaces. Comput. Aided Geom. Des. (2016), http://dx.doi.org/10.1016/j.cagd.2016.06.005

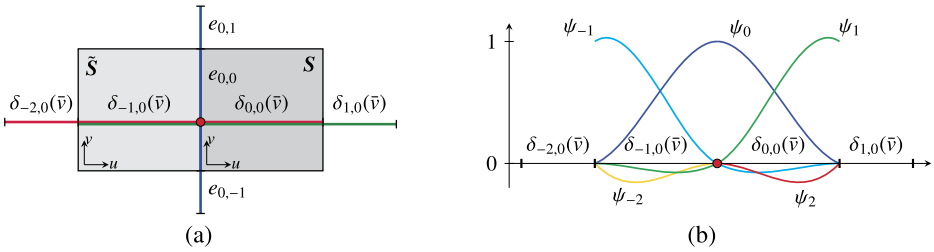

Fig. 5. A class of fundamental functions with $w = 4$. (a) Local parameter vectors at the boundary point $(0, \bar{v})$ and $(1, \bar{v})$ respectively for the patches $\boldsymbol{S}$ and $\tilde{\boldsymbol{S}}$ involved in the proof of Proposition 2; (b) Fundamental functions defined on the corresponding parameter intervals in the cross-boundary direction.

Using the last two above identities, at any boundary point equation (16) reduces to

$$\frac{\partial^r}{\partial u^r}\boldsymbol{S}(u,v)\Big|_{(0,v)} = \sum_{i=-\frac{w}{2}+1}^{\frac{w}{2}-1}\sum_{j=-\frac{w}{2}+1}^{\frac{w}{2}} \boldsymbol{p}_{i,j}\,\psi_j\Big(v e_{0,0}, \boldsymbol{e}(0)\Big)\,\frac{\partial^r}{\partial u^r}\psi_i\Big(u\delta_{0,0}(v), \boldsymbol{d}(v)\Big)\Big|_{(0,v)}. \tag{19}$$

We now turn to considering the neighboring surface patch $\tilde{\boldsymbol{S}}$. Denoted $\tilde{\boldsymbol{d}}(v)$ and $\tilde{\boldsymbol{e}}(u)$ the local parameter vectors for $\tilde{\boldsymbol{S}}$, we have

$$\tilde{\boldsymbol{d}}(v) = \Big(\delta_{-\frac{w}{2},0}(v), \ldots, \delta_{-1,0}(u), \ldots, \delta_{\frac{w}{2}-2,0}(v)\Big), \qquad \tilde{\boldsymbol{e}}(u) = \Big(\epsilon_{-1,-\frac{w}{2}+1}(u), \ldots, \epsilon_{-1,0}(u), \ldots, \epsilon_{-1,\frac{w}{2}-1}(u)\Big), \tag{20}$$

and thus

$$\frac{\partial^r}{\partial u^r}\tilde{\boldsymbol{S}}(u,v) = \sum_{i=-\frac{w}{2}}^{\frac{w}{2}-1}\sum_{j=-\frac{w}{2}+1}^{\frac{w}{2}} \boldsymbol{p}_{i,j}\sum_{q=0}^{r}\binom{r}{q}\frac{\partial^q}{\partial u^q}\psi_i\Big(u\delta_{-1,0}(v), \tilde{\boldsymbol{d}}(v)\Big)\,\frac{\partial^{r-q}}{\partial u^{r-q}}\psi_j\Big(v\epsilon_{-1,0}(u), \tilde{\boldsymbol{e}}(u)\Big).$$

As before, it can easily be verified that

$$\frac{\partial^{r-q}}{\partial u^{r-q}}\psi_j\Big(v\epsilon_{-1,0}(u), \tilde{\boldsymbol{e}}(u)\Big)\Big|_{(1,v)} = 0, \qquad q = 0, \ldots, r-1, \qquad r = 1, \ldots, k.$$

Moreover, from the compact support of the fundamental functions follows that

$$\frac{\partial^r}{\partial u^r}\psi_{-\frac{w}{2}}\Big(u\delta_{-1,0}(v), \tilde{\boldsymbol{d}}(v)\Big)\Big|_{(1,v)} = 0, \qquad r = 1, \ldots, k,$$

and, observing that $\boldsymbol{e}(0) = \tilde{\boldsymbol{e}}(1)$, we obtain

$$\frac{\partial^r}{\partial u^r}\tilde{\boldsymbol{S}}(u,v)\Big|_{(1,v)} = \sum_{i=-\frac{w}{2}+1}^{\frac{w}{2}-1}\sum_{j=-\frac{w}{2}+1}^{\frac{w}{2}} \boldsymbol{p}_{i,j}\,\psi_j\Big(v e_{0,0}, \boldsymbol{e}(0)\Big)\,\frac{\partial^r}{\partial u^r}\psi_i\Big(u\delta_{-1,0}(v), \tilde{\boldsymbol{d}}(v)\Big)\Big|_{(1,v)}. \tag{21}$$

Now, in view of (19) and (21), it only remains to show that the derivatives of order $r = 1, \ldots, k$ of the functions ψ_i agree after the scaling $\Delta(v)$ in (14).

Comparing the expressions in (17) and (20) we can see that the two vectors $\boldsymbol{d}(v)$ and $\tilde{\boldsymbol{d}}(v)$ are one a "shifted" version of the other and therefore "overlap" almost everywhere, with the exception of the first element in $\tilde{\boldsymbol{d}}$ and the last one in $\boldsymbol{d}$ (Fig. 5(a) schematizes the situation for a class of fundamental functions having support width $w = 4$). These two different intervals are uninfluential to the value and derivatives of the fundamental functions at a boundary point (see Fig. 5(b)). As a consequence, at such a point, the fundamental functions defined on $\boldsymbol{d}(v)$ and $\tilde{\boldsymbol{d}}(v)$ agree together with their derivatives up to order k, namely

$$\frac{\partial^r}{\partial x^r}\psi_i(x, \boldsymbol{d}(v))\Big|_{x=0} = \frac{\partial^r}{\partial x^r}\psi_i(x, \tilde{\boldsymbol{d}}(v))\Big|_{x=\delta_{-1,0}(v)}, \qquad i = -\frac{w}{2}-1, \ldots, \frac{w}{2}+1, \qquad r = 0, \ldots, k.$$

The last relation and (15) entail that

$$\frac{\partial^r}{\partial u^r}\boldsymbol{S}(u,v)\Big|_{(0,v)} = \left(\frac{\delta_{0,0}(v)}{\delta_{-1,0}(v)}\right)^r \frac{\partial^r}{\partial u^r}\tilde{\boldsymbol{S}}(u,v)\Big|_{(1,v)},$$

which concludes the proof. □

Please cite this article in press as: Antonelli, M., et al. High quality local interpolation by composite parametric surfaces. Comput. Aided Geom. Des. (2016), http://dx.doi.org/10.1016/j.cagd.2016.06.005

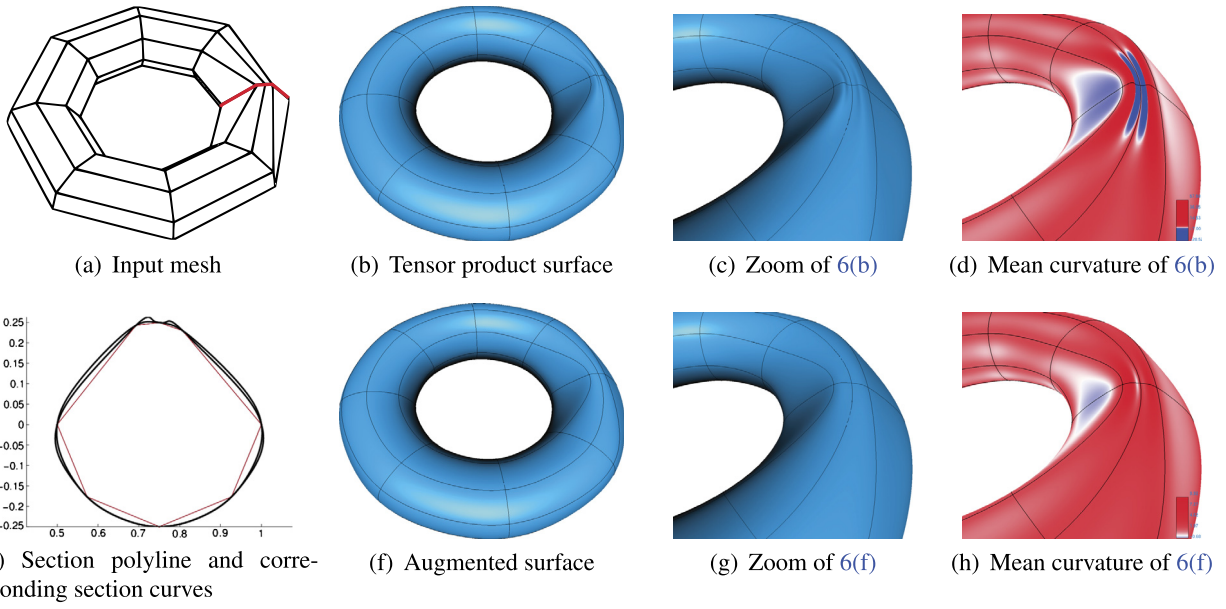

(a) Input mesh (b) Tensor product surface (c) Zoom of 6(b) (d) Mean curvature of 6(b)

(e) Section polyline and corresponding section curves (f) Augmented surface (g) Zoom of 6(f) (h) Mean curvature of 6(f)

Fig. 6. Comparison between tensor product and augmented surfaces built upon univariate splines of class $D^5C^2P^2S^4$. Fig. 6(e) shows the interpolatory curves of the considered class generated from the red-colored section polyline in 6(a) with augmented and tensor product parameterizations. (For interpretation of the references to color in this figure, the reader is referred to the web version of this article.)

3.1. Examples

This section presents some examples of augmented surfaces, which will allow us to highlight several important features of the proposed method. In particular:

- Augmented surfaces show significantly better quality with respect to tensor product ones. In fact, when the data points are unevenly distributed, tensor product surfaces show unwanted interpolation artifacts. According to our experiments, these artifacts are not present in their augmented counterpart.
- For each class $D^gC^kP^mS^w$ of local, univariate, non-uniform splines in Beccari et al. (2013a), Antonelli et al. (2014), we get an augmented surface with the same smoothness and support width, and where the section curves are univariate splines in the given class. This yields a large family of surfaces with different properties. Thanks to the augmented parametrization, each of these surfaces is aesthetically pleasing and faithfully resembles the input mesh.
- Even in the case where a tensor product surface has no artifacts, its augmented counterpart better approximates the shape of the input mesh.

In the following we discuss the above points in more detail, also with the help of graphical illustrations.

As a premise, we shall recall that the method for computation of the edge parameter intervals greatly impacts the surface shape and its quality. Therefore, to allow a fair comparison, all our examples are based on the same technique. Comparing different approaches of curve parametrization is not the scope of this paper. The reader may refer to Fang and Hung (2013) for a recent study on the topic.

For the augmented surfaces, the edge parameter intervals are computed through the centripetal parametrization as illustrated in the previous section. Moreover, tensor product surfaces are parameterized by averaging the centripetal parameter interval values, in such a way that every isocurve can have the same (non-uniform) parameter sequence. Note that, in this case, a different parameter sequence is created for each domain direction. For brevity, we call this approach a *mean parametrization*.

Fig. 6 shows two surfaces obtained by interpolating a "modified" torus mesh with augmented and mean parameterization. Due to the uneven length of mesh edges, finding a good quality interpolating surface is a challenging task. In fact, the tensor product surface shows noticeable ripples both in the shaded display and in the mean curvature graph. In contrast, these artifacts are not encountered in the augmented surface, which is aesthetically pleasing and exhibits a better curvature graph.

A closer examination of one section polyline (in red in Fig. 6(a)) will help us in understanding the different behavior of the two surfaces. Fig. 6(e) depicts the section curves obtained when the parameter intervals are generated by the augmented and mean parametrizations. The averaging step required by the mean parametrization entails that the parameter intervals assigned to the edges of the considered polyline are very different than the initial centripetal parametrization and have little relationship with the geometry of the interpolation data. This is responsible for the undesired ripple. Oppositely, in the

Please cite this article in press as: Antonelli, M., et al. High quality local interpolation by composite parametric surfaces. Comput. Aided Geom. Des. (2016), http://dx.doi.org/10.1016/j.cagd.2016.06.005

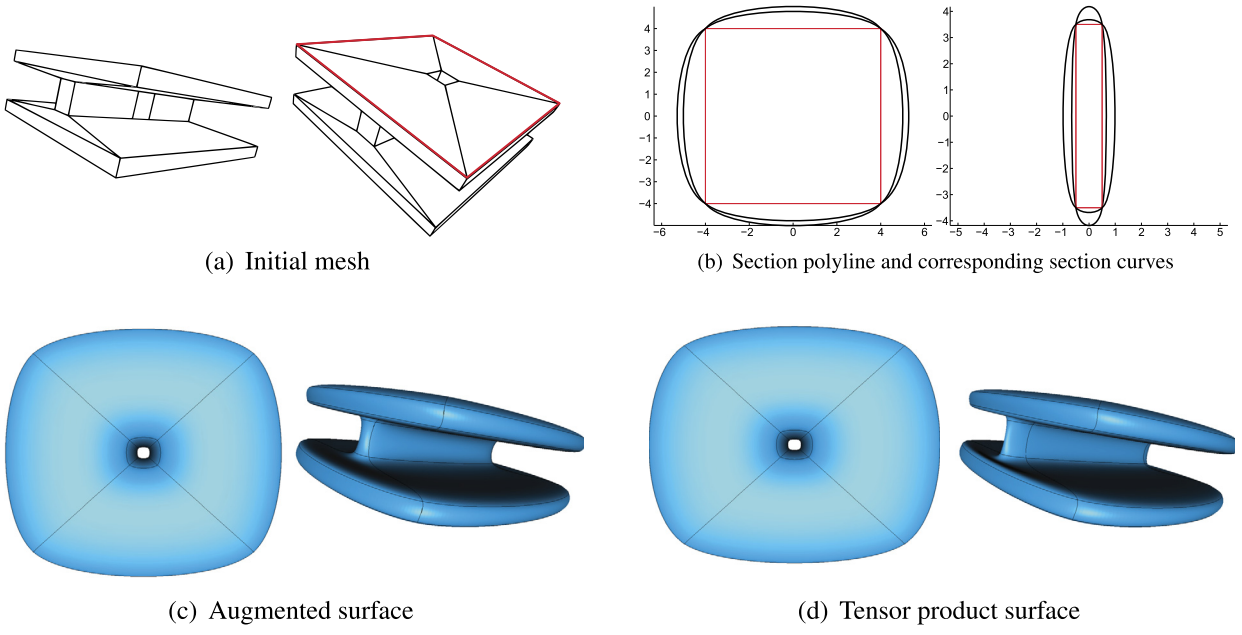

Fig. 7. Comparison between augmented and tensor product surface. (a) Input mesh; (b) The section polyline highlighted in (a) and section curves of class $D^5C^2P^2S^4$, with the augmented (centripetal) and mean parametrizations. (c)–(d) Corresponding augmented and tensor product surfaces. (For interpretation of the references to color in this figure, the reader is referred to the web version of this article.)

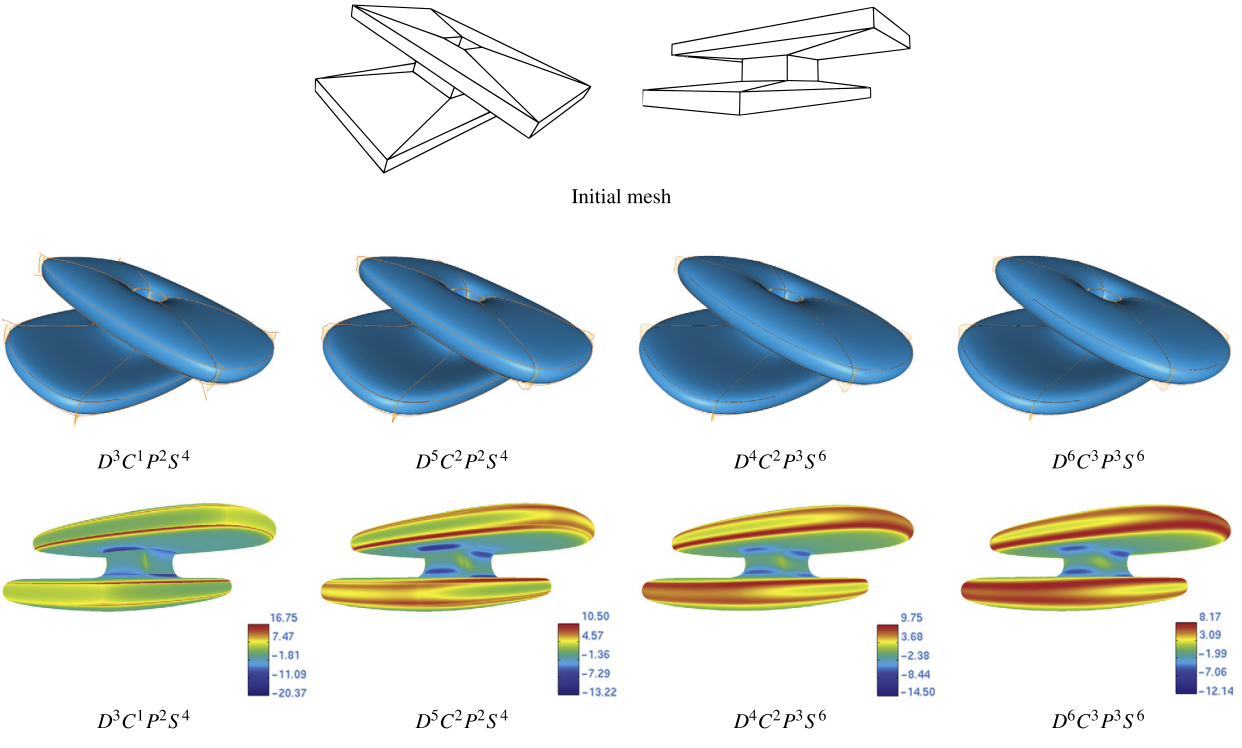

Fig. 8. Local interpolatory surfaces with augmented parametrization built upon different classes of univariate splines $D^gC^kP^mS^w$ (g, k, m and w are the degree, order of continuity, maximum degree of polynomials that are reproduced and support width). 1st row: Input mesh depicted from two different points of view; 2nd row: Surfaces and curvature combs of section curves superimposed; 3rd row: Mean curvature.

augmented surface, the section polyline vertices are interpolated at centripetal parameters and the resulting section curve is free of shape artifacts.

Fig. 12 (for now restricted to cases 12(a) and 12(b)) is another example where the mean parametrization fails compared to the augmented one. The tensor product surface with mean parametrization self intersects, whereas no artifact is present

Please cite this article in press as: Antonelli, M., et al. High quality local interpolation by composite parametric surfaces. Comput. Aided Geom. Des. (2016), http://dx.doi.org/10.1016/j.cagd.2016.06.005

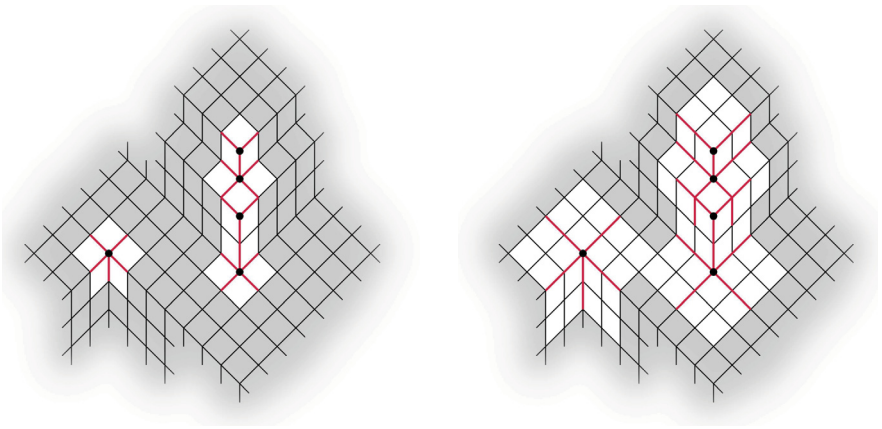

(a) w=4 (b) w=6

Fig. 9. Mesh containing several extraordinary vertices. The regular regions are highlighted in grey for support width $w = 4$ and $w = 6$.

in the augmented surface. We shall use this example also to recall that local interpolation easily allows for managing open surfaces. In the considered case, an additional layer of mesh faces is generated by linear extrapolation across the boundary. With these additional data, the boundary patches can straightforwardly be computed by formula (10).

The example in Fig. 7 emphasizes that an augmented surface may be preferable compared to a tensor product surface, even when the latter does not present unwanted artifacts. The red-colored section polyline in Fig. 7(a) is a regular square. The symmetry in the data is reflected in the corresponding section curve of the augmented surface (Fig. 7(b)). Conversely, this is not the case with the tensor product surface, as a side effect of the underlying mean parametrization. Therefore, even if both surfaces are G^2 continuous and free of interpolation artifacts, the augmented one more faithfully resembles the input data.

Fig. 8 shows local interpolatory surfaces with augmented parametrization based upon various classes $D^g C^k P^m S^w$. Regardless of the different properties of the underlying fundamental functions, all the displayed surfaces are aesthetically pleasing and closely resemble the shape of the input mesh. The difference between one surface and another is made apparent by the curvature comb of the section curves and by the mean curvature graph. In view of Proposition 3, the displayed surfaces are G^k continuous with $k = 1, 2, 3$, according to the continuity of the class $D^g C^k P^m S^w$.

4. Local interpolation of meshes with extraordinary vertices by augmented surface patches

In this section we discuss how to generate local interpolatory surfaces of high quality when the input mesh contains extraordinary vertices. To this aim, we shall partition the mesh into *regular* and *extraordinary regions*. Regular regions comprise all the mesh faces where the local method described in Section 3 applies, whereas the remaining faces will form extraordinary regions. The generation of an augmented surface patch of the form (10) requires that we can uniquely determine a surrounding rectangular grid of mesh vertices, whose size depends on the support of the patch. In particular, we need a $w \times w$ vertex grid, when the underlying fundamental functions belong to class $D^g C^k P^m S^w$. We say that a patch is *regular* when it can be generated by formula (10), whereas it is *extraordinary* otherwise. Fig. 9 illustrates the regular and extraordinary regions of a sample mesh for $w = 4, 6$. As shown in the figure, we do not require that extraordinary vertices be separated by (a sufficient number of) regular ones. As a consequence, if the support width is greater than 4, an extraordinary patch may not contain an extraordinary vertex.

After constructing regular augmented patches wherever possible, we obtain a surface with "holes" surrounding the extraordinary vertices. For example, in the case of support width 4 or 6, around each isolated extraordinary vertex we will have a hole corresponding to one ring or two rings of mesh faces respectively. Moreover, the boundaries of the augmented regular patches will form a network of open curves of class $D^g C^k P^m S^w$. Therefore, the problem to be addressed is how to patch the extraordinary regions of the mesh with sufficient smoothness and how to properly manage the join between regular and extraordinary patches, taking into account the underlying augmented parametrization.

Our construction for the extraordinary patches is based on the well-known Coons–Gregory scheme, which we will tweak in order to conform to the augmented parametrization. To explain the basic idea, we start by considering the G^1 Coons–Gregory patches (Gregory, 1974) (see also the classical text books (Hoschek and Lasser, 1993; Farin, 2002)), which can be more familiar to the majority of readers. Successively, we also address the G^2 form of these patches, initially proposed in Miura and Wang (1991) and later developed in Hermann (1996). As a result, depending on the method used, an extraordinary patch will join with G^1 or G^2 continuity the neighboring patches, that can be either regular or extraordinary. At the same time, as we have seen in the previous section, the regular portion of the surface will have arbitrary smoothness G^k away from the boundary between the regular and extraordinary regions.

Please cite this article in press as: Antonelli, M., et al. High quality local interpolation by composite parametric surfaces. Comput. Aided Geom. Des. (2016), http://dx.doi.org/10.1016/j.cagd.2016.06.005

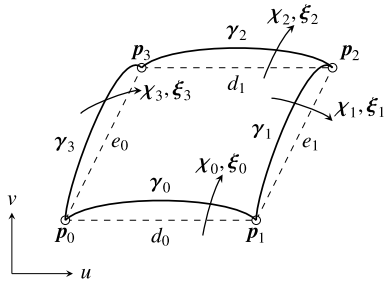

Fig. 10. Schematic representation of the quantities needed for the definition of an augmented Coons–Gregory patch (the second-order cross-derivative fields $\boldsymbol{\xi}_i$ are needed for the biquintically blended patch only).

We remark that the entire method is not intended for meshes that are mainly composed of extraordinary vertices (although applicable also in this case). In fact, the regular portion of the composite surface should serves as a "guide" for the generation of the extraordinary patches.

The input data for a Coons–Gregory patch are 4 boundary curves and the related cross-boundary derivative fields (in short *cross-derivatives*) of the first and, possibly, second order. Each of the 4 boundaries may join either an extraordinary patch or a regular one. In the former situation, the boundary curve and cross-derivatives need to be prescribed in an appropriate way and how to do so is an independent issue. Therefore, from now we assume that this information is given. We will return on the problem of determining the missing boundary information in Section 4.3, where we discuss how these data have been generated in our prototype system.

When the boundary joins a regular patch of the form (10), the input data are sampled from such a patch and we need to take into account that the cross-derivatives vary according to the augmented parametrization. More precisely, the transversal derivatives of an augmented patch depend on the local parametrization functions and, according to Lemma 2, the mapping from the uv domain to the local variables x, y is different at each boundary point. The two following subsections are devoted to illustrating how a Coons–Gregory patch needs to be defined in order to correctly interpolate the data sampled from an augmented regular patch.

Before delving into details, we introduce the setting and notation. As in Section 3, we assume that a parameter interval value is assigned to every mesh edge, both in the regular regions and in the extraordinary ones. This is reasonable, since an automatic parametrization method generally yields a parameter interval in both cases. For instance, if we wish to use the centripetal parametrization, formula (6) applies regardless of whether an edge belongs in a regular region or not. Consequently, the parameter intervals associated with the edges of an extraordinary face may not form a rectangle. This yields an augmented parametrization for the extraordinary patches as well. We denote an augmented extraordinary patch by $\boldsymbol{S}^*$, to distinguish it from the regular patches so far denoted by $\boldsymbol{S}$.

Fig. 10 illustrates the labeling of the relevant quantities needed to construct an augmented Coons–Gregory patch. We adopt a simplified notation with respect to the preceding part of the paper. The face vertices to be interpolated are now denoted by $\boldsymbol{p}_i$, $i = 1, \ldots, 4$ and sometimes we shall call these points the *corners*. The boundary curves are denoted by $\boldsymbol{\gamma}_i$, $i = 1, \ldots, 4$ and $\boldsymbol{\chi}_i, \boldsymbol{\xi}_i$ represent the respective first and second order cross-derivative fields. Moreover, d_0, d_1, e_0 e_1 are the edge parameter intervals.

With an extraordinary patch, we associate the parametric domain $[0, 1]^2$ and two local parametrization functions $\delta(v)$ and $\epsilon(u)$, $u, v \in [0, 1]$, following the same definition in Section 3. More precisely, with the current notation, formulae (7a)–(7b) read as follows: $\delta(v)$ is the polynomial $\delta : [0, 1] \to [d_0, d_1]$ of degree $2k + 1$ such that $\delta(0) = d_0$, $\delta(1) = d_1$ and $\delta^{(r)}(0) = \delta^{(r)}(1) = 0$, $r = 1, \ldots, k$. Analogously, $\epsilon(u)$ is the polynomial $\epsilon : [0, 1] \to [e_0, e_1]$ of degree $2k+1$ such that $\epsilon(0) = e_0$, $\epsilon(1) = e_1$ and $\epsilon^{(r)}(0) = \epsilon^{(r)}(1) = 0$, $r = 1, \ldots, k$.

We describe the boundary curves in terms of the local variables

$$x_0 = ud_0, \qquad x_1 = ud_1, \qquad y_0 = ve_0, \qquad y_1 = ve_1, \tag{22}$$

in such a way that each boundary segment $\boldsymbol{\gamma}_i$, is parameterized on the corresponding edge parameter interval. This means that $\boldsymbol{\gamma}_0(x_0) = \boldsymbol{p}_0$ when $x_0 = 0$ and $\boldsymbol{\gamma}_0(x_0) = \boldsymbol{p}_1$ when $x_0 = d_0$, with similar interpolation conditions for the other three curves $\boldsymbol{\gamma}_1(y_1)$, $\boldsymbol{\gamma}_2(x_1)$, $\boldsymbol{\gamma}_3(y_0)$.

4.1. Augmented bicubically blended Coons patches with Gregory correction

For the construction of a G^1 Coons–Gregory patch, we shall use the cubic Hermite basis on $[0, 1]$, arranged in the vector

$$\boldsymbol{H}(u) = \left(-1, 2u^3 - 3u^2 + 1, -2u^3 + 3u^2, u^3 - 2u^2 + u, u^3 - u^2\right)^T.$$

We define the augmented Coons–Gregory patch $\boldsymbol{S}^*$ as

$$\boldsymbol{S}^*(u, v) = -\boldsymbol{H}(u)^T M_3(u, v) \boldsymbol{H}(v),$$

Please cite this article in press as: Antonelli, M., et al. High quality local interpolation by composite parametric surfaces. Comput. Aided Geom. Des. (2016), http://dx.doi.org/10.1016/j.cagd.2016.06.005

where

$$M_3(u,v)=\begin{pmatrix} 0 & \boldsymbol{\gamma}_0(x_0) & \boldsymbol{\gamma}_2(x_1) & \epsilon(u)\,\boldsymbol{\chi}_0(x_0) & \epsilon(u)\,\boldsymbol{\chi}_2(x_1)\\ \boldsymbol{\gamma}_3(y_0) & \boldsymbol{p}_0 & \boldsymbol{p}_3 & e_0\,\boldsymbol{\gamma}_3'(0) & e_0\,\boldsymbol{\gamma}_3'(e_0)\\ \boldsymbol{\gamma}_1(y_1) & \boldsymbol{p}_1 & \boldsymbol{p}_2 & e_1\,\boldsymbol{\gamma}_1'(0) & e_1\,\boldsymbol{\gamma}_1'(e_1)\\ \delta(v)\,\boldsymbol{\chi}_3(y_0) & d_0\,\boldsymbol{\gamma}_0'(0) & d_1\,\boldsymbol{\gamma}_2'(0) & \multicolumn{2}{c}{\multirow{2}{*}{$\Omega_{1,1}$}}\\ \delta(v)\,\boldsymbol{\chi}_1(y_1) & d_0\,\boldsymbol{\gamma}_0'(d_0) & d_1\,\boldsymbol{\gamma}_2'(d_1) & & \end{pmatrix}, \tag{23}$$

for any $(u,v)\in[0,1]^2$, being ϵ and δ the related local parametrization functions and x_0, x_1, y_0, y_1 determined by (22).

The choice of expressing the cross-derivative fields in terms of the local variables x_i and y_i, $i=0,1$, facilitates the construction of the augmented Coons–Gregory patch in the case where the boundary information is not available from an adjacent regular patch, and thus needs to be heuristically estimated, as, in this case, it is more natural to specify the missing fields in the local variables.

As a consequence of the augmented parametrization, a suitable scaling factor is associated with the entries of the patch matrix M_3 to guarantee that the correct derivatives are interpolated both in the boundary and cross-boundary direction. More precisely, the derivatives of the boundary curves, $\boldsymbol{\gamma}_i'$, $i=1,\dots,4$, are mapped to the uv domain multiplying their value by the length of the related parameter interval d_i or e_i, $i=0,1$. In addition, in view of Proposition 1, the scaling factor needed to express the first derivatives $\boldsymbol{\chi}_0(x_0), \boldsymbol{\chi}_1(y_1), \boldsymbol{\chi}_2(x_1), \boldsymbol{\chi}_3(y_0)$ in the uv domain corresponds to the value of the appropriate local parametrization function at the evaluation point (u,v). Therefore, whereas the scaling factor is constant for the derivatives of the boundary curves, for the cross-derivatives it changes at each (u,v). Finally, we shall also take into account that, when $\boldsymbol{\chi}_i$ is sampled from a regular augmented patch $\boldsymbol{S}$, then its value needs to be divided by the appropriate local parametrization function before being inserted in (23).

To complete the definition of the matrix (23), we need to provide the twist vectors matrix $\Omega_{1,1}$, possibly with *Gregory correction* for twist incompatibility. This is given by

$$\Omega_{1,1}:=\begin{pmatrix} d_0e_0\,\frac{u\boldsymbol{\chi}_3'(0)+v\boldsymbol{\chi}_0'(0)}{u+v} & d_1e_0\,\frac{u\boldsymbol{\chi}_3'(e_0)+(1-v)\boldsymbol{\chi}_2'(0)}{u+(1-v)}\\ d_0e_1\,\frac{(1-u)\boldsymbol{\chi}_1'(0)+v\boldsymbol{\chi}_0'(d_0)}{(1-u)+v} & d_1e_1\,\frac{(1-u)\boldsymbol{\chi}_1'(e_1)+(1-v)\boldsymbol{\chi}_2'(d_1)}{(1-u)+(1-v)} \end{pmatrix},$$

where the scaling factors of type d_ie_j, $i,j=0,1$ preceding the rational terms are determined by the same argument used above. It can be shown through direct verification that the patch $\boldsymbol{S}^*$ interpolates the corner points, the boundary curves and the cross-boundary first derivatives. Therefore the resulting composite surface is G^1 continuous at the boundaries between regular and extraordinary regions and in the interior of the latter. This type of continuity is sufficient when the regular regions are constructed from C^1 fundamental functions, like in the case of Catmull–Rom splines. Otherwise, it may be desirable to use a patching scheme with higher continuity as discussed in the next subsection.

4.2. Augmented biquintically blended Coons patches with Gregory correction

In order to construct a G^2 Coons–Gregory patch we exploit the quintic Hermite basis, arranged in the vector

$$\begin{aligned}\boldsymbol{H}(u)=\Big(&-1,-6u^5+15u^4-10u^3+1,6u^5-15u^4+10u^3,-3u^5+8u^4-6u^3+u,\\ &-3u^5+7u^4-4u^3,-\frac{1}{2}u^5+\frac{3}{2}u^4-\frac{3}{2}u^3+\frac{1}{2}u^2,\frac{1}{2}u^5-u^4+\frac{1}{2}u^3\Big)^T,\end{aligned}$$

and we compute the value of the augmented patch $\boldsymbol{S}^*$ according to

$$\boldsymbol{S}^*(u,v)=-\boldsymbol{H}(u)^TM_5(u,v)\boldsymbol{H}(v).$$

The patch matrix is now

$$M_5(u,v)=\left(\begin{array}{ccc|cc} \multicolumn{3}{c|}{\multirow{2}{*}{$M_3(u,v)$}} & \epsilon^2(u)\,\boldsymbol{\xi}_0(x_0) & \epsilon^2(u)\,\boldsymbol{\xi}_2(x_1)\\ & & & e_0^2\,\boldsymbol{\gamma}_3''(0) & e_0^2\,\boldsymbol{\gamma}_3''(e_0)\\ & & & e_1^2\,\boldsymbol{\gamma}_1''(0) & e_1^2\,\boldsymbol{\gamma}_1''(e_1)\\ \hline \delta^2(v)\,\boldsymbol{\xi}_3(y_0) & d_0^2\,\boldsymbol{\gamma}_0''(0) & d_1^2\,\boldsymbol{\gamma}_2''(0) & \multicolumn{2}{c}{\multirow{2}{*}{$\Omega_{1,2}$}}\\ \delta^2(v)\,\boldsymbol{\xi}_1(y_1) & d_0^2\,\boldsymbol{\gamma}_0''(d_0) & d_1^2\,\boldsymbol{\gamma}_2''(d_1) & & \\ \multicolumn{2}{c}{\multirow{2}{*}{$\Omega_{2,1}$}} & & \multicolumn{2}{c}{\multirow{2}{*}{$\Omega_{2,2}$}}\\ & & & & \end{array}\right),$$

where M_3 is given by (23) and $\boldsymbol{\xi}_0(x_0), \boldsymbol{\xi}_1(y_1), \boldsymbol{\xi}_2(x_1), \boldsymbol{\xi}_3(y_0)$ are the cross-boundary second derivatives. The mixed derivatives matrices, possibly with Gregory correction for twist incompatibility, are defined as follows:

Please cite this article in press as: Antonelli, M., et al. High quality local interpolation by composite parametric surfaces. Comput. Aided Geom. Des. (2016), http://dx.doi.org/10.1016/j.cagd.2016.06.005

$$\Omega_{1,1} = \begin{pmatrix} d_0 e_0 \frac{u^2 \boldsymbol{\chi}_3'(0) + v^2 \boldsymbol{\chi}_0'(0)}{u^2+v^2} & d_1 e_0 \frac{u^2 \boldsymbol{\chi}_3'(e_0) + (1-v)^2 \boldsymbol{\chi}_2'(0)}{u^2+(1-v)^2} \\ d_0 e_1 \frac{(1-u)^2 \boldsymbol{\chi}_1'(0) + v^2 \boldsymbol{\chi}_0'(d_0)}{(1-u)^2+v^2} & d_1 e_1 \frac{(1-u)^2 \boldsymbol{\chi}_1'(e_1) + (1-v)^2 \boldsymbol{\chi}_2'(d_1)}{(1-u)^2+(1-v)^2} \end{pmatrix},$$

$$\Omega_{1,2} = \begin{pmatrix} d_0 e_0^2 \frac{u^2 \boldsymbol{\chi}_3''(0) + v^2 \boldsymbol{\xi}_0'(0)}{u^2+v^2} & d_1 e_0^2 \frac{u^2 \boldsymbol{\chi}_3''(e_0) + (1-v)^2 \boldsymbol{\xi}_2'(0)}{u^2+(1-v)^2} \\ d_0 e_1^2 \frac{(1-u)^2 \boldsymbol{\chi}_1''(0) + v^2 \boldsymbol{\xi}_0'(d_0)}{(1-u)^2+v^2} & d_1 e_1^2 \frac{(1-u)^2 \boldsymbol{\chi}_1''(e_1) + (1-v)^2 \boldsymbol{\xi}_2'(d_1)}{(1-u)^2+(1-v)^2} \end{pmatrix},$$

$$\Omega_{2,1} = \begin{pmatrix} d_0^2 e_0 \frac{u^2 \boldsymbol{\xi}_3'(0) + v^2 \boldsymbol{\chi}_0''(0)}{u^2+v^2} & d_1^2 e_0 \frac{u^2 \boldsymbol{\xi}_3'(e_0) + (1-v)^2 \boldsymbol{\chi}_2''(0)}{u^2+(1-v)^2} \\ d_0^2 e_1 \frac{(1-u)^2 \boldsymbol{\xi}_1'(0) + v^2 \boldsymbol{\chi}_0''(d_0)}{(1-u)^2+v^2} & d_1^2 e_1 \frac{(1-u)^2 \boldsymbol{\xi}_1'(e_1) + (1-v)^2 \boldsymbol{\chi}_2''(d_1)}{(1-u)^2+(1-v)^2} \end{pmatrix},$$

$$\Omega_{2,2} = \begin{pmatrix} d_0^2 e_0^2 \frac{u^2 \boldsymbol{\xi}_3''(0) + v^2 \boldsymbol{\xi}_0''(0)}{u^2+v^2} & d_1^2 e_0^2 \frac{u^2 \boldsymbol{\xi}_3''(e_0) + (1-v)^2 \boldsymbol{\xi}_2''(0)}{u^2+(1-v)^2} \\ d_0^2 e_1^2 \frac{(1-u)^2 \boldsymbol{\xi}_1''(0) + v^2 \boldsymbol{\xi}_0''(d_0)}{(1-u)^2+v^2} & d_1^2 e_1^2 \frac{(1-u)^2 \boldsymbol{\xi}_1''(e_1) + (1-v)^2 \boldsymbol{\xi}_2''(d_1)}{(1-u)^2+(1-v)^2} \end{pmatrix}.$$

The interpretation of the construction and of the scaling factors that appear in M_5 is conceptually similar to what we have seen in the preceding subsection and therefore no additional comment is needed. As before, the terms involving second order derivatives require appropriate scaling to map the local variables x, y to the uv domain and again the proper scaling factor can be determined from relation (15). It can be shown through direct verification that the patch $\boldsymbol{S}^*$ interpolates the corner points, the boundary curves and the cross-boundary first and second derivatives. Therefore it guarantees that the resulting composite surface is G^2 continuous at the boundaries between regular and extraordinary regions and in the interior of the latter.

4.3. Mesh regions with extraordinary vertices and G^1/G^2 compatibility conditions

The construction of a Coons–Gregory patch requires boundary curves and cross-derivative fields. When this information cannot be sampled from an existing regular patch, then it shall be drawn from the mesh itself, which represents the only available data. In this section we will focus on how to specify the boundary curves. Being these computed, the cross-derivative fields can be constructed by suitable interpolation of the boundary curves values and derivatives at the corners according to standard procedures (see Farin, 2002 and Hermann, 1996 for the G^1 and G^2 case respectively).

Methods to create fair curve networks from arbitrary meshes were suggested in Moreton and Séquin (1994), and, to the best of our knowledge, this is the only available reference on the subject. Our case is different, however, since much of the curve network is created using the local interpolating univariate splines $D^g C^k P^m S^w$ and there only remains to define isolated segments of the network.

For meshes that contain extraordinary vertices, we extend the definition of a section polyline given is Section 3. A section polyline is now a sequence of adjacent edges characterized in one of the following ways: i) it is closed and all its vertices are regular or ii) it is open, the first and last points are extraordinary vertices and all the remaining vertices are regular. Accordingly, a section curve is one that interpolates the vertices of a section polyline. The section curves starting or ending at the extraordinary vertices can be thought off as open curves.

Wherever possible, we wish to construct the patch boundary segments in such a way that, globally, the related section curve belongs to class $D^g C^k P^m S^w$. Using this condition, if $w > 4$, some of the missing curve segments can directly be determined by locally interpolating the corresponding section polyline. For example, with reference to Fig. 9, only the red-colored edges cannot be computed in this way.

When they can not be otherwise determined, we construct the boundary segments by polynomial interpolation of endpoints and endpoint derivatives. The latter shall be sampled from existing curve segments when available, in such a way that the corresponding section curve has globally the correct continuity. Otherwise they need to be heuristically estimated. In doing so, we shall take into account that the derivatives at one vertex need to satisfy G^k, $k = 1, 2$ compatibility conditions (depending on the continuity of the Coons–Gregory patch), meaning that locally the resulting network of section curves can be embedded into a C^k surface. In particular, G^1 compatibility entails that all the curve tangents lie on the same plane, which is the tangent plane. Conditions for G^2 compatibility are more complex and do not have a direct geometric interpretation (Hermann, 1996; Hermann et al., 2012).

Our approach for generating G^1 and G^2 compatible derivatives is based on least squares polynomial approximation. This idea is not new, as was already used, for example, to tweak the derivatives of Catmull–Clark subdivision surfaces in the neighborhood of extraordinary vertices (Antonelli et al., 2013). The outline of the procedure is as follows. First, a proper set of points in the vicinity of the extraordinary vertex is generated. These points should serve as a "guide" for the shape of the surface that we want to fit. Then a least squares polynomial approximating these points is computed and its derivatives are sampled along proper directions. To make the numerical examples reproducible, the details of our implementation are provided in Appendix B. The described method guarantees G^2 compatibility and, in our tests, has always generated visually pleasing surfaces in the vicinity of the extraordinary vertices. One can reasonably expect that even better results can be produced by more elaborate techniques and further investigation is a possible topic for future research.

Please cite this article in press as: Antonelli, M., et al. High quality local interpolation by composite parametric surfaces. Comput. Aided Geom. Des. (2016), http://dx.doi.org/10.1016/j.cagd.2016.06.005

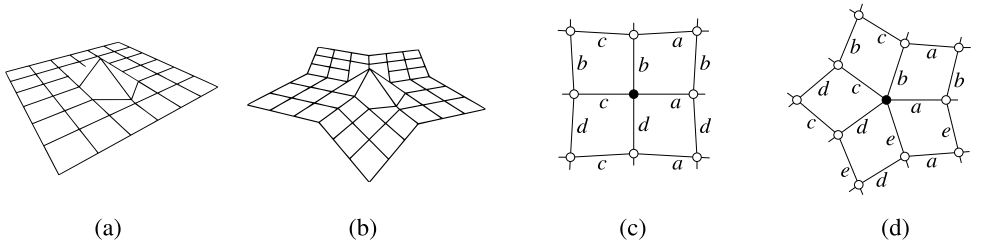

Fig. 11. (a) A regular mesh and (b) a mesh with an extraordinary vertex of valence 5. (c)–(d) Corresponding mean parametrization in the neighborhood of the central vertex: each letter indicates a different edge parameter interval value.

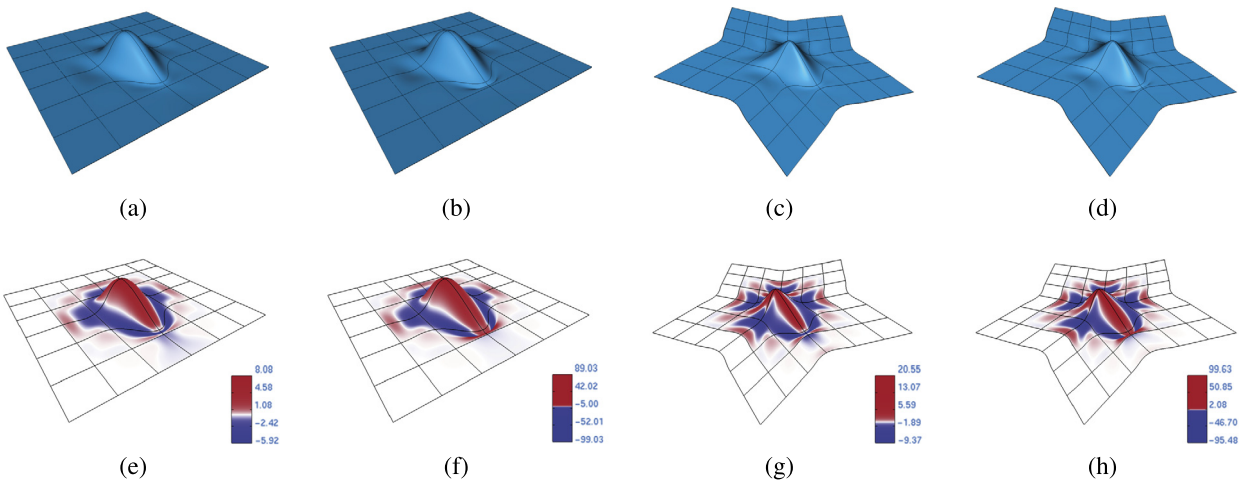

Fig. 12. First line: surfaces from the class $D^5C^2P^2S^4$ interpolating the meshes in Figs. 11(a) and 11(b) with augmented parametrization ((a) and (c)) and mean parametrization ((b) and (d)). Second line: corresponding mean curvature graph.

4.4. Examples

In this section we present some examples of augmented surfaces interpolating meshes with extraordinary vertices. The displayed surfaces are based upon the class of univariate splines $D^5C^2P^2S^4$, which offers a good tradeoff between high continuity (the corresponding surfaces are G^2 continuous) and small support width (and thus higher computational efficiency).

Following the same outline of the regular case examples discussed in Section 3.1, we start by comparing surfaces generated through the augmented and mean parameterizations. For meshes with extraordinary vertices, the mean parametrization can be generalized as suggested in Cashman et al. (2009). In particular, one parameter interval is assigned to every edge belonging in the same edge ribbon and it is defined as the average of all parameter intervals in the ribbon. This strategy results in the configuration illustrated in Fig. 11(d) and obviously generalizes the setting of parameters used in the regular case.

Fig. 12 emphasizes that, also for surfaces containing extraordinary vertices, the mean parametrization may give rise to noticeable artifacts, which can be overcome by the use of the augmented parametrization. The different result of the two parameterizations is readily apparent from the shaded display and is further emphasized by the curvature graph.

Fig. 13 presents more complex examples of G^2-continuous surfaces of high quality with augmented parametrization. Figs. 13(b) and 13(f) show the regular patches and the constructed network of section curves. As discussed in the previous section, the section curves passing through the extraordinary vertices can be thought off as open curves. The curve segments emanating from the extraordinary vertices are determined as a degree 5 polynomials, interpolating endpoint values and derivatives up to second order. As a result, the entire section curves belong to class $D^5C^2P^2S^4$. The augmented Coons–Gregory patches are illustrated in Figs. 13(c) and 13(g), whereas Figs. 13(d) and 13(h) show the entire composite surface. For the open surface depicted in Fig. 13, the boundary patches are regular augmented patches of the form (10). Their construction is performed by suitably extrapolating the mesh across the boundary in order to obtain an additional layer of faces and vertices.

Fig. 14 compares the results of the augmented and mean parameterizations for the meshes in Fig. 13 and emphasizes the better quality of the augmented surfaces. In particular, in the extraordinary region, the surface curvature produced by the mean parametrization wiggles several times between positive and negative values, while this does not happen when the augmented parametrization is used.

Please cite this article in press as: Antonelli, M., et al. High quality local interpolation by composite parametric surfaces. Comput. Aided Geom. Des. (2016), http://dx.doi.org/10.1016/j.cagd.2016.06.005

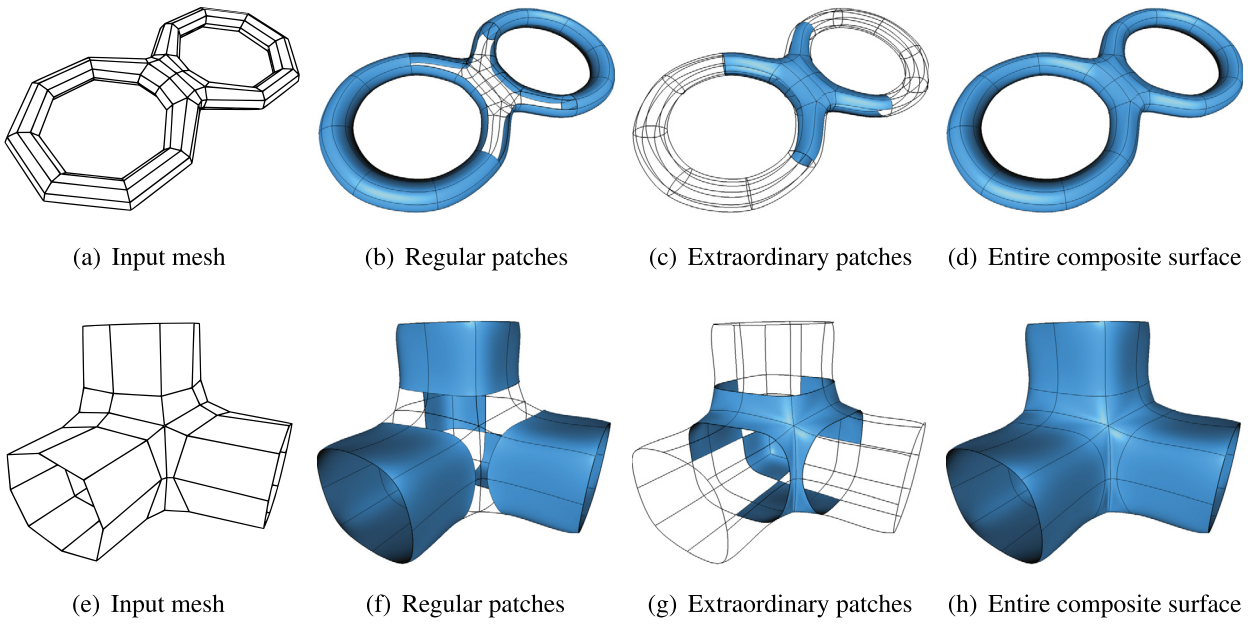

(a) Input mesh (b) Regular patches (c) Extraordinary patches (d) Entire composite surface

(e) Input mesh (f) Regular patches (g) Extraordinary patches (h) Entire composite surface

Fig. 13. Surfaces from the class $D^5C^2P^2S^4$ with augmented parametrization.

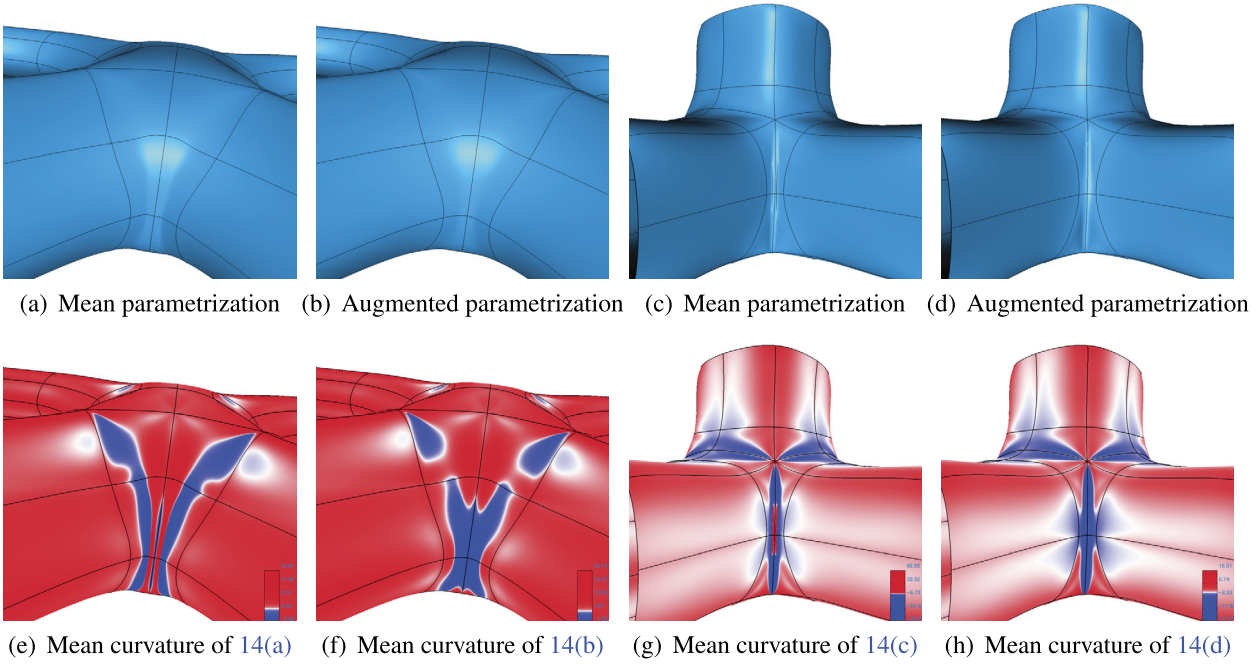

(a) Mean parametrization (b) Augmented parametrization (c) Mean parametrization (d) Augmented parametrization

(e) Mean curvature of 14(a) (f) Mean curvature of 14(b) (g) Mean curvature of 14(c) (h) Mean curvature of 14(d)

Fig. 14. Zoom of the surfaces obtained from the meshes in Fig. 13 with augmented and mean parametrization.

Finally, Fig. 15 comprises some challenging data sets and the corresponding augmented interpolatory surfaces, which are globally G^2, free of unwanted artifacts and overall approximate in a reasonable way the shape of the input mesh. We consider this result highly nontrivial for a local interpolation method.

5. Conclusion

We have presented a local construction for interpolatory composite surfaces, which is based on the use of univariate spline interpolants having degree g, continuity C^k, polynomial reproduction degree m and support width w. Thanks to the augmented parametrization, each section curve is parameterized independently of the others and in the most appropriate way. Away from the extraordinary vertices the generated surfaces retain the same smoothness of the underlying class of

Please cite this article in press as: Antonelli, M., et al. High quality local interpolation by composite parametric surfaces. Comput. Aided Geom. Des. (2016), http://dx.doi.org/10.1016/j.cagd.2016.06.005

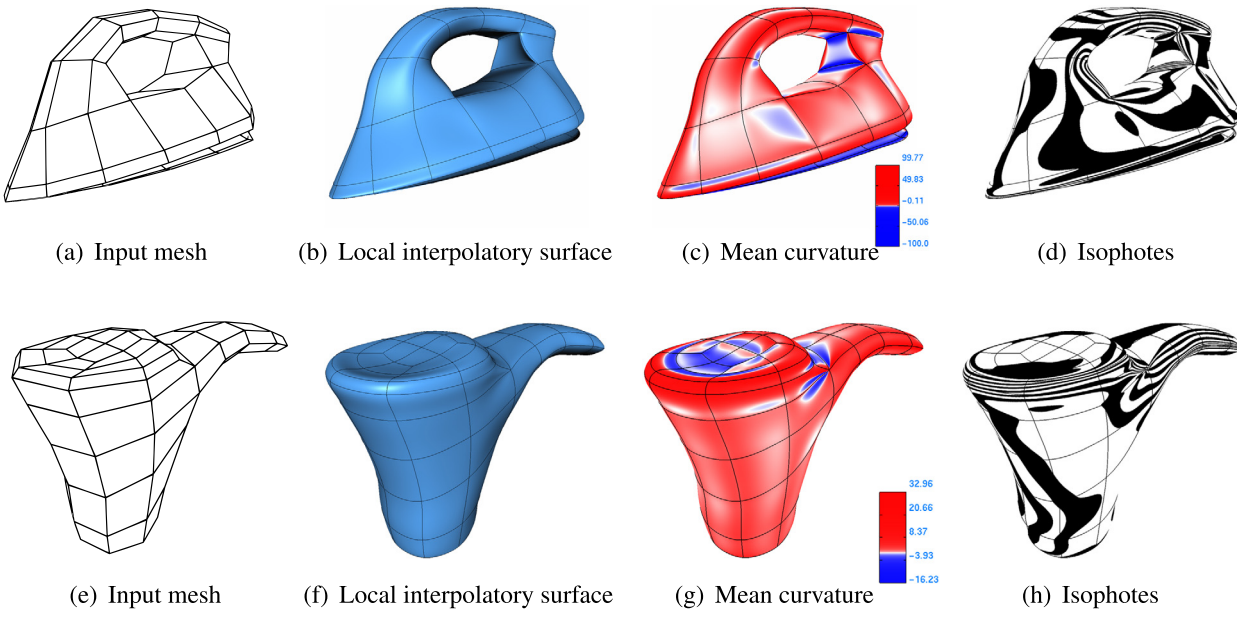

(a) Input mesh (b) Local interpolatory surface (c) Mean curvature (d) Isophotes

(e) Input mesh (f) Local interpolatory surface (g) Mean curvature (h) Isophotes

Fig. 15. Surfaces from the class $D^5C^2P^2S^4$ with augmented parameterization.

univariate splines. Surface regions surrounding extraordinary vertices have been generated by means of a modified form of Coons–Gregory patches, joining with G^1 or G^2 continuity the regular portion of the surface. The obtained surfaces are aesthetically well-behaved, as we have demonstrated by several numerical examples concerning both regular and extraordinary meshes.

We postpone to a future work a more thorough investigation of other possible methods for patching extraordinary vertices. Using the augmented parametrization in different contexts is another topic worthy of consideration. For example, there is no problem (in principle) in applying the augmented parametrization with standard B-splines, and its extension to more general techniques of surface generation may also be of interest.

Acknowledgements

This research was supported by the European Eurostars project NIIT4CAD http://eurostars.unibo.it/ and by the Italian INdAM National Group for Scientific Calculus (GNCS).

Appendix A. Some classes of fundamental functions

The following fundamental spline functions are obtained following the approach reported in Beccari et al. (2013a).

A.1. Fundamental functions of the class $D^3C^1P^2S^4$

Recalling our notation $d_i = x_{i+1} - x_i$, in the interval $[-d_{i-2} - d_{i-1}, d_i + d_{i+1}]$ the expression of the fundamental function ψ_i is given by

$$\psi_i(x) = \begin{cases} \dfrac{(d_{i-1}+x)\,(d_{i-2}+d_{i-1}+x)^2}{d_{i-2}d_{i-1}\,(d_{i-2}+d_{i-1})}, & -d_{i-2}-d_{i-1} \le x < -d_{i-1}, \\ \dfrac{(d_{i-1}+x)\left(d_i\left(-x^2+d_{i-1}d_{i-2}+d_{i-1}^2\right)-x\,(d_{i-2}+d_{i-1})\,(d_{i-1}+x)\right)}{d_{i-1}^2 d_i\,(d_{i-2}+d_{i-1})}, & -d_{i-1} \le x < 0, \\ \dfrac{(d_i-x)\left(-x^2(d_{i-1}+d_i+d_{i+1})+xd_i\,(d_i+d_{i+1})+d_{i-1}d_i\,(d_i+d_{i+1})\right)}{d_{i-1}d_i^2\,(d_i+d_{i+1})}, & 0 \le x < d_i, \\ \dfrac{(d_i-x)\,(d_i+d_{i+1}-x)^2}{d_i d_{i+1}\,(d_i+d_{i+1})}, & d_i \le x \le d_i + d_{i+1}. \end{cases}$$

The local parameter vector associated with $[x_s, x_{s+1}]$ is $\boldsymbol{d} = (d_{s-1}, d_s, d_{s+1})$ and for any $x \in [0, d_s]$ the four nonzero fundamental functions ψ_i, $i = s-1, \ldots, s+2$ have the expression

Please cite this article in press as: Antonelli, M., et al. High quality local interpolation by composite parametric surfaces. Comput. Aided Geom. Des. (2016), http://dx.doi.org/10.1016/j.cagd.2016.06.005

$$\psi_{s-1}(x;\boldsymbol{d}) = -\frac{x\,(x-d_s)^2}{d_{s-1}d_s\,(d_{s-1}+d_s)},$$
$$\psi_s(x;\boldsymbol{d}) = \frac{1}{d_s^2}\,(x-d_s)\left(\frac{x^2}{d_s+d_{s+1}} + \frac{x\,(x-d_s)}{d_{s-1}} - d_s\right),$$
$$\psi_{s+1}(x;\boldsymbol{d}) = \frac{1}{d_s^2}x\left(\frac{d_s\,(d_{s-1}+2x)-x^2}{d_{s-1}+d_s} - \frac{x\,(x-d_s)}{d_{s+1}}\right),$$
$$\psi_{s+2}(x;\boldsymbol{d}) = \frac{x^2\,(x-d_s)}{d_s d_{s+1}\,(d_s+d_{s+1})}.$$

A.2. Fundamental functions of the class $D^5C^2P^2S^4$

Recalling our notation $d_i = x_{i+1} - x_i$, in the interval $[-d_{i-2}-d_{i-1}, d_i+d_{i+1}]$ the expression of the fundamental function ψ_i is given by

$$\psi_i(x) = \begin{cases} -\dfrac{(d_{i-1}+x)\,(d_{i-2}+d_{i-1}+x)^3\,(-d_{i-2}+2d_{i-1}+2x)}{d_{i-2}^3 d_{i-1}\,(d_{i-2}+d_{i-1})}, \\ \quad -d_{i-2}-d_{i-1} \le x < -d_{i-1}, \\ \dfrac{d_i\,(d_{i-1}+x)\left(3x^3 d_{i-1} + d_{i-1}^3\,(d_{i-2}+d_{i-1}) + 2x^4\right) - x\,(d_{i-2}+d_{i-1})\,(d_{i-1}-2x)\,(d_{i-1}+x)^3}{d_{i-1}^4 d_i\,(d_{i-2}+d_{i-1})}, \\ \quad -d_{i-1} \le x < 0, \\ \dfrac{(d_i-x)\left((d_{i-1}+d_i+d_{i+1})\,(2x^4-3x^3d_i) + x d_i^3\,(d_i+d_{i+1}) + d_{i-1}d_i^3\,(d_i+d_{i+1})\right)}{d_{i-1}d_i^4\,(d_i+d_{i+1})}, \\ \quad 0 \le x < d_i, \\ -\dfrac{(x-d_i)\,(-2d_i+d_{i+1}+2x)\,(d_i+d_{i+1}-x)^3}{d_i d_{i+1}^3\,(d_i+d_{i+1})}, \\ \quad d_i \le x \le d_i+d_{i+1}. \end{cases}$$

The local parameter vector associated with $[x_s, x_{s+1}]$ is $\boldsymbol{d} = (d_{s-1}, d_s, d_{s+1})$ and for any $x \in [0, d_s]$ the four nonzero fundamental functions ψ_i, $i = s-1, \ldots, s+2$ have the expression

$$\psi_{s-1}(x;\boldsymbol{d}) = \frac{x\,(x-d_s)^3\,(d_s+2x)}{d_{s-1}d_s^3\,(d_{s-1}+d_s)},$$
$$\psi_s(x;\boldsymbol{d}) = \frac{(d_s-x)\left(d_{s-1}\left(-3x^3d_s + d_s^4 + d_s^3 d_{s+1} + 2x^4\right) + x\,(d_s+d_{s+1})\,(d_s+2x)\,(x-d_s)^2\right)}{d_{s-1}d_s^4\,(d_s+d_{s+1})},$$
$$\psi_{s+1}(x;\boldsymbol{d}) = \frac{1}{d_s^4}x\left(\frac{x^2\,(2x-3d_s)\,(x-d_s)}{d_{s+1}} + \frac{-5x^3d_s + 3x^2d_s^2 + d_s^3\,(d_{s-1}+x) + 2x^4}{d_{s-1}+d_s}\right),$$
$$\psi_{s+2}(x;\boldsymbol{d}) = -\frac{x^3\,(2x-3d_s)\,(x-d_s)}{d_s^3 d_{s+1}\,(d_s+d_{s+1})}.$$

Appendix B. Derivatives generation

Let $\boldsymbol{p}_0$ be a vertex of valence n where we want to compute a set of G^1 or G^2 compatible derivatives. In this section, we denote by $\boldsymbol{p}_i$, $i = 1, \ldots, n$, the endpoints of the edges emanating from $\boldsymbol{p}_0$, by d_i the parameter intervals of the edges $\overline{\boldsymbol{p}_0\boldsymbol{p}_i}$ and by $\boldsymbol{f}_i$ the vectors $\boldsymbol{p}_i - \boldsymbol{p}_0$.

With each edge $\overline{\boldsymbol{p}_0\boldsymbol{p}_i}$ we associate a vector $\boldsymbol{T}_{\boldsymbol{p}_0,\boldsymbol{p}_i}$ defined as

$$\boldsymbol{T}_{\boldsymbol{p}_0,\boldsymbol{p}_i} = \frac{\alpha_i}{d_i}\boldsymbol{f}_i - \frac{1-\alpha_i}{\bar{d}_i}\overline{\boldsymbol{f}}_i, \tag{B.1}$$

where

$$\alpha_i = \frac{\bar{d}_i}{d_i + \bar{d}_i}, \qquad \bar{d}_i = -\sum_{\substack{j=1 \\ j\neq i}}^{n} \cos\left(\frac{2\pi(j-i)}{n}\right) d_j, \qquad \overline{\boldsymbol{f}}_i = \sum_{\substack{j=1 \\ j\neq i}}^{n} \left|\cos\left(\frac{2\pi(j-i)}{n}\right)\right| \boldsymbol{f}_j. \tag{B.2}$$

When $n = 4$, equation (B.1) reduces to the well-known Bessel estimate for computing an approximation of the first derivative of a parametric curve (Farin, 2002, Section 9.8). For a general valence $n \neq 4$, $\boldsymbol{T}_{\boldsymbol{p}_0,\boldsymbol{p}_i}$ represents a heuristic estimate of the first derivative at $\boldsymbol{p}_0$ of the curve segment between $\boldsymbol{p}_0$ and $\boldsymbol{p}_i$. In particular, we can observe that, when n is even and the points $\boldsymbol{p}_i$ have rotational symmetry with respect to $\boldsymbol{p}_0$, then $\boldsymbol{T}_{\boldsymbol{p}_0,\boldsymbol{p}_i}$ corresponds to the Bessel formula applied to the three points $\boldsymbol{p}_{i+\frac{n}{2}}, \boldsymbol{p}_0, \boldsymbol{p}_i$, which are intuitively associated with a curve passing through $\boldsymbol{p}_0$.

At this point, if only G^1 compatibility is required, we can simply get an appropriate set of derivatives at $\boldsymbol{p}_0$ by projecting the vectors $\boldsymbol{T}_{\boldsymbol{p}_0,\boldsymbol{p}_i}$, $i = 1, \ldots, n$ on a common plane.

We will now proceed to determine a G^2 compatible set of derivatives. In particular, let $\boldsymbol{\tau}^{(1)}_{\boldsymbol{p}_0,\boldsymbol{p}_i}$ and $\boldsymbol{\tau}^{(2)}_{\boldsymbol{p}_0,\boldsymbol{p}_i}$ be respectively the first and second derivative of the curve segment associated with the edge $\overline{\boldsymbol{p}_0\boldsymbol{p}_i}$. Our strategy is to construct a polynomial $\boldsymbol{P}$ that interpolates $\boldsymbol{p}_0$ and approximates in a least-squares sense a suitable set of points $\boldsymbol{q}_j$, $j = 1, \ldots, 2n$ around $\boldsymbol{p}_0$ and set $\boldsymbol{\tau}^{(1)}_{\boldsymbol{p}_0,\boldsymbol{p}_i}$ and $\boldsymbol{\tau}^{(2)}_{\boldsymbol{p}_0,\boldsymbol{p}_i}$ as the derivatives of such polynomial along proper directions. The approximation points $\boldsymbol{q}_j$ are chosen so that the polynomial $\boldsymbol{P}$ will have a reasonable shape in a small neighborhood of $\boldsymbol{p}_0$. In particular, for each $i = 1, \ldots, n$, $\boldsymbol{q}_i$ and $\boldsymbol{q}_{n+i}$ are respectively the values at parameters $\frac{d_i}{4}$ and $\frac{d_i}{2}$ of the cubic polynomial $\boldsymbol{\lambda}$ such that $\boldsymbol{\lambda}(0) = \boldsymbol{p}_0$, $\boldsymbol{\lambda}'(0) = \boldsymbol{T}_{\boldsymbol{p}_0,\boldsymbol{p}_i}$, $\boldsymbol{\lambda}(d_i) = \boldsymbol{p}_i$, $\boldsymbol{\lambda}'(d_i) = \boldsymbol{T}_{\boldsymbol{p}_i,\boldsymbol{p}_0}$. Note that the vector $\boldsymbol{T}_{\boldsymbol{p}_i,\boldsymbol{p}_0}$ represents a derivative at $\boldsymbol{p}_i$, and thus it shall be sampled from the adjacent segment of the section curve passing through $\boldsymbol{p}_i$ and $\boldsymbol{p}_0$, when this is available, or otherwise computed from formulae (B.1)–(B.2).

We exploit a bivariate polynomial $\boldsymbol{P}$ of degree 3 or 2 respectively in the case $n \geq 5$ or $n = 3, 4$. The coefficients of $\boldsymbol{P}$ are determined componentwise by minimizing the expression

$$\sum_{j=1}^{2n} \left(\boldsymbol{P}(x_j, y_j) - \boldsymbol{q}_j\right)^2,$$

where the parametric coordinates (x_j, y_j) associated with the point $\boldsymbol{q}_j$ are given by

$$(x_j, y_j) = r_j(\cos\eta_i, \sin\eta_i), \quad j = i, n+i, \tag{B.3}$$

and the angles $\eta_i, i = 1, \ldots, n$ are obtained by mapping onto the xy plane the spatial configuration formed by the angles $\zeta_i := \widehat{\boldsymbol{T}_{\boldsymbol{p}_0,\boldsymbol{p}_i}, \boldsymbol{T}_{\boldsymbol{p}_0,\boldsymbol{p}_{i+1}}}$, $i = 1, \ldots, n$, namely

$$\eta_1 = 0, \qquad \eta_i = \eta_{i-1} + \zeta_i \frac{2\pi}{\sum_{j=1}^{n} \zeta_j}, \quad i = 2, \ldots, n.$$

The value of r_j in (B.3) is a free parameter and can be exploited to locally tune the shape of the surface. When the edge parameter intervals d_i are computed according to (6), then a possible choice (which we have used in the proposed examples) is

$$r_j = \left\|\boldsymbol{q}_j - \boldsymbol{p}_0\right\|_2^{\alpha}.$$

Finally, we can set $\boldsymbol{\tau}^{(1)}_{\boldsymbol{p}_0,\boldsymbol{p}_i}$ and $\boldsymbol{\tau}^{(2)}_{\boldsymbol{p}_0,\boldsymbol{p}_i}$, $i = 1, \ldots, n$, to be the first and the second derivatives of $\boldsymbol{P}$ at $\boldsymbol{p}_0$ in the direction determined by η_i.

References

Ahlberg, J.H., Nilson, E.N., Walsh, J.L., 1967. The Theory of Splines and Their Applications. Mathematics in Science and Engineering, vol. 38. Academic Press, New York, NY, USA.

Antonelli, M., Beccari, C.V., Casciola, G., 2014. A general framework for the construction of piecewise-polynomial local interpolants of minimum degree. Adv. Comput. Math. 40. http://dx.doi.org/10.1007/s10444-013-9335-y.

Antonelli, M., Beccari, C.V., Casciola, G., Ciarloni, R., Morigi, S., 2013. Subdivision surfaces integrated in a CAD system. Comput. Aided Des. 45, 1294–1305. http://dx.doi.org/10.1016/j.cad.2013.06.007.

Beccari, C.V., Casciola, G., Romani, L., 2013a. Construction and characterization of non-uniform local interpolating polynomial splines. J. Comput. Appl. Math. 240, 5–19. http://dx.doi.org/10.1016/j.cam.2012.06.025.

Beccari, C.V., Casciola, G., Romani, L., 2013b. Non-uniform non-tensor product local interpolatory subdivision surfaces. Comput. Aided Geom. Des. 30, 357–373. http://dx.doi.org/10.1016/j.cagd.2013.02.002.

Becerra Sagredo, J., 2003. Z-splines: moment conserving cardinal spline interpolation of compact support for arbitrarily spaced data. Technical report no. 2003-10.

Blu, T., Thévenaz, P., Unser, M., 2003. Complete parameterization of piece-wise-poly-nomial interpolation kernels. IEEE Trans. Image Process. 12, 1297–1309. http://dx.doi.org/10.1109/TIP.2003.818018.

Cashman, T.J., Augsdörfer, U.H., Dodgson, N.A., Sabin, M.A., 2009. NURBS with extraordinary points: high-degree, non-uniform, rational subdivision schemes. ACM Trans. Graph. 28 (46), 1–9. http://dx.doi.org/10.1145/1531326.1531352.

Catmull, E., Rom, R., 1974. A class of local interpolating splines. In: Barnhill, R.E., Riesenfeld, R.F. (Eds.), Computer Aided Geometric Design. Academic Press, New York, NY, USA, pp. 317–326.

Please cite this article in press as: Antonelli, M., et al. High quality local interpolation by composite parametric surfaces. Comput. Aided Geom. Des. (2016), http://dx.doi.org/10.1016/j.cagd.2016.06.005

Chui, C.K., De Villiers, J.M., 1996. Applications of optimally local interpolation to interpolatory approximations and compactly supported wavelets. Math. Comput. 65, 99–114. http://dx.doi.org/10.1090/S0025-5718-96-00672-2.

Fang, J.J., Hung, C.L., 2013. An improved parameterization method for B-spline curve and surface interpolation. Comput. Aided Des. 45, 1005–1028. http://dx.doi.org/10.1016/j.cad.2013.01.005.

Farin, G., 2002. Curves and Surfaces for CAGD: A Practical Guide, 5th ed.. Morgan Kaufmann Publishers Inc., San Francisco, CA, USA.

Farin, G., Hoschek, J., Kim, M.S. (Eds.), 2002. Handbook of Computer Aided Geometric Design. Elsevier Science Publishers B. V., Amsterdam, The Netherlands.

Floater, M.S., 2008. On the deviation of a parametric cubic spline interpolant from its data polygon. Comput. Aided Geom. Des. 25, 148–156. http://dx.doi.org/10.1016/j.cagd.2007.08.001.

Foley, T.A., Nielson, G.M., 1989. Knot selection for parametric spline interpolation. In: Lyche, T., Schumaker, L.L. (Eds.), Mathematical Methods in Computer Aided Geometric Design.

Gregory, J.A., 1974. Smooth interpolation without twist constraints. In: Riesenfeld, R.E., Barnhill, R.F. (Eds.), Computer Aided Geometric Design. Academic Press, pp. 71–87.

Han, X., 2011. A class of general quartic spline curves with shape parameters. Comput. Aided Geom. Des. 28, 151–163. http://dx.doi.org/10.1016/j.cagd.2011.02.001.

Hermann, T., 1996. G^2 interpolation of free form curve networks by biquintic Gregory patches. Comput. Aided Geom. Des. 13, 873–893. http://dx.doi.org/10.1016/S0167-8396(96)00013-1.

Hermann, T., Peters, J., Strotman, T., 2012. Curve networks compatible with G^2 surfacing. Comput. Aided Geom. Des. 29, 219–230.

Hoschek, J., Lasser, D., 1993. Fundamentals of Computer Aided Geometric Design. A. K. Peters, Ltd.

Karčiauskas, K., Peters, J., 2015. Improved shape for multi-surface blends. Graph. Models 82, 87–98. http://dx.doi.org/10.1016/j.gmod.2015.06.006. URL: http://www.sciencedirect.com/science/article/pii/S1524070315000259.

Lee, E.T.Y., 1989. Choosing nodes in parametric curve interpolation. Comput. Aided Des. 21, 363–370. http://dx.doi.org/10.1016/0010-4485(89)90003-1.

Loop, C., Schaefer, S., 2008. G^2 tensor product splines over extraordinary vertices. Comput. Graph. Forum 27, 1373–1382. http://dx.doi.org/10.1111/j.1467-8659.2008.01277.x.

Miura, K., Wang, K., 1991. C^2 Gregory patch. In: Post, F., Barth, W. (Eds.), EUROGRAPHICS '91, pp. 481–492.

Moreton, H.P., Séquin, C.H., 1994. Minimum variation curves and surfaces for computer-aided geometric design. In: Sapidis, N.S. (Ed.), Designing Fair Curves and Surfaces. SIAM, pp. 123–159.

Müller, K., Fünfzig, C., Reusche, L., Hansford, D., Farin, G., Hagen, H., 2010. DINUS: double insertion, nonuniform, stationary subdivision surfaces. ACM Trans. Graph. 29 (25), 1–21. http://dx.doi.org/10.1145/1805964.1805969.

Müller, K., Reusche, L., Fellner, D., 2006. Extended subdivision surfaces: building a bridge between NURBS and Catmull–Clark surfaces. ACM Trans. Graph. 25, 268–292. http://dx.doi.org/10.1145/1138450.1138455.

Perters, J., 2002. Geometric continuity. In: Farin, G., Hoschek, J., Kim, M.S. (Eds.), Handbook of Computer Aided Geometric Design. Elsevier Science Publishers B. V., Amsterdam, The Netherlands, pp. 193–227.

Prautzsch, H., 1997. Freeform splines. Comput. Aided Geom. Des. 14, 201–206. http://dx.doi.org/10.1016/S0167-8396(96)00029-5. URL: http://www.sciencedirect.com/science/article/pii/S0167839696000295.

Salvi, P., Várady, T., 2014. G^2 surface interpolation over general topology curve networks. Comput. Graph. Forum 33, 151–160. http://dx.doi.org/10.1111/cgf.12483.

Salvi, P., Várady, T., Rockwood, A., 2014. Ribbon-based transfinite surfaces. Comput. Aided Geom. Des. 31, 613–630. http://dx.doi.org/10.1016/j.cagd.2014.06.006.

Sederberg, T.W., Zheng, J., Sewell, D., Sabin, M.A., 1998. Non-uniform recursive subdivision surfaces. In: Proceedings of the 25th Annual Conference on Computer Graphics and Interactive Techniques. ACM, pp. 387–394.

Ueno, T., Truscott, S., Okada, M., 2007. New spline basis functions for sampling approximations. Numer. Algorithms 45. http://dx.doi.org/10.1007/s11075-007-9119-x.

Várady, T., Rockwood, A., Salvi, P., 2011. Transfinite surface interpolation over irregular n-sided domains. Comput. Aided Des. 43, 1330–1340.

Yuksel, C., Schaefer, S., Keyser, J., 2011. Parameterization and applications of Catmull–Rom curves. Comput. Aided Des. 43, 747–755. http://dx.doi.org/10.1016/j.cad.2010.08.008.

Please cite this article in press as: Antonelli, M., et al. High quality local interpolation by composite parametric surfaces. Comput. Aided Geom. Des. (2016), http://dx.doi.org/10.1016/j.cagd.2016.06.005